Structural studies of activated parkin and its binding partners

Chin Chia (George) Sung

Department of Biochemistry

McGill University, Montreal

A thesis submitted to McGill University in partial fulfillment of the requirements of the degree of Master of Science

Table of Contents

Abstract	4
Résumé	5
Author Contribution	8
List of Abbreviations	9
List of Figures	11
1. Introduction	12
1.1 Parkinson's Disease (PD)	12
1.2 Pathology of PD	13
1.3 Ubiquitination Pathway	15
1.4 Types of Ubiquitin E3 ligases	18
1.6 Parkin as an RBR E3 Ligase	21
1.7 Parkin activation	22
2. Material and Methods	24
2.1 Primer Used	24
2.2 Construct Used	24
2.3 Cloning, expression, and purification of recombinant proteins in <i>E. coli</i>	25
2.4 Phosphorylation of parkin complex and ubiquitin	26
2.5 Autoubiquitination assays of rat parkin	2.7

	2.6 Crystallization	. 28
	2.7 Data collection and structure determination	. 28
	2.8 Sortase A reactions	. 29
	2.9 NMR experiments	. 30
	2.10 Hydrogen-deuterium exchange mass spectrometry (HDX-MS)	. 30
	2.11 UbVS assay	. 32
	2.12 Data Availability	. 32
3.	Results	. 33
	3.1 Crystallization of activated parkin	. 33
	3.2 Structural analysis of activated parkin	. 38
	3.3 Ubl phosphorylation is important for activation	. 43
	3.4 Resolving conflicting models of Parkin activation	. 46
	3.5 Parkin phosphorylation is required to free up RING2	. 47
4.	Discussion	. 53
5.	References	. 59

Abstract

Parkinson's Disease (PD) is the second most common neurodegenerative disorder, affecting around 100,000 Canadians. About 15% of the documented cases are shown to be inherited and usually leads to an early onset of the disease. One of the genes involved in the familial autosomal recessive form of PD is the *PARK2* gene, which encodes for the protein, parkin is a ubiquitin E3 ligase that is involved in the mitochondria quality control with the help from PINK1, a mitochondrial targeted kinase.

Parkin and the PINK1 regulate a quality control system for mitochondria. In its basal state, parkin is auto-inhibited by intra-molecular interaction preventing the binding to E2-conjugating enzyme and access to the catalytic cysteine. In order to activate parkin, PINK1 phosphorylates ubiquitin on the outer membrane of damaged mitochondria, leading to parkin recruitment and activation via phosphorylation of its ubiquitin-like (Ubl) domain. Previously, the mechanism in which phosphorylation of the Ubl domain leads to parkin's activation was unclear. However, we were able to crystallize the activated form of parkin which allow us to describe the mechanism of parkin activation by phosphorylation.

The crystal structure of phosphorylated fruit fly parkin in complex with phosphorylated ubiquitin and an E2 ubiquitin-conjugating enzyme reveals the key activating step is the movement of the Ubl domain and release of the catalytic RING2 domain. Hydrogen-deuterium exchange and NMR experiments with the various intermediates in the activation pathway confirm and extend the interpretation of the crystal structure to mammalian parkin. Our results rationalize previously unexplained Parkinson's disease mutations and the presence of internal linkers that allow large domain movements in parkin.

Résumé

La maladie de Parkinson (MP) est la deuxième maladie neurodégénérative la plus populaire, touchant environ 100 000 Canadiens. Environ 15% des cas documentés sont d'origine héréditaire et conduisent généralement à un début précoce de la maladie. L'un des gènes impliqués dans la forme familiale autosomale récessive de la MP est le gène *PARK2*, qui code pour la protéine parkin. Parkin est une ligase d'ubiquitine E3 impliquée dans le contrôle de la qualité des mitochondries à l'aide de PINK1, une kinase mitochondriale.

À l'état basal, la parkin est auto-inhibée par des interactions intramoléculaires limitant sa liaison à l'enzyme de conjugaison E2 et l'accès de sa cystéine catalytique. Dans les mitochondries endommagées, PINK1 phosphoryle l'ubiquitine présente sur la membrane externe, ce qui entraîne le recrutement, puis l'activation de la parkin via la phosphorylation de son domaine de type ubiquitine (Ubl). Jusqu'à présent, le mécanisme moléculaire par lequel la phosphorylation du domaine Ubl conduisait à l'activation de parkin n'était pas connu. Nous avons donc décidé de cristalliser la forme activée de la parkin afin de proposer un mécanisme d'activation de la parkin par sa phosphorylation.

La structure cristallographique de la protéine parkin phosphorylée de la mouche à fruits, en complexe avec de l'ubiquitine phosphorylée et une enzyme de conjugaison de l'ubiquitine E2, révèle que l'élément-clé de l'activation est la relocalisation du domaine Ubl et le détachement du domaine catalytique RING2. Des expériences d'échange hydrogène-deutérium et de résonance magnétique nucléaire avec différents intermédiaires de la voie d'activation ont confirmé l'information tirée de notre structure cristallographique et prouvé qu'elle pouvait être extrapolée aux protéines parkin des mammifères. Nos résultats ont permis d'élucider pourquoi certaines

mutations inexpliqueés jusqu'à maintenant, pouvaient causer la maladie de Parkinson et le rôle de lieurs internes qui permettent le réarrangement des différents domaines de parkin.

Acknowledgement

There are many people to acknowledge for their help and support. Without them, I would not be able to complete this thesis and to advance the project. The four years I have spent with these colleagues and friends shaped me as a structural biologist and researcher. I am very grateful to have each and every one of you in my life to help guide me and make the lab a pleasant work environment.

Firstly, I would like to thank Dr. Kalle Gehring for accepting me into his lab and providing me with the opportunity to work on the parkin project. I am very grateful to Dr. Marjan Seirafi for the training that was required to carry out different experiments during my undergraduate degree. I would like to thank Dr. Véronique Sauvé for the supervision during my undergraduate Honour's project and Master's project. Her advice in X-ray crystallography helped me crystallize and solve the structure of activated parkin, which is the main focus of this thesis. I would like to thank Dr. Jean-François Trempe for his expertise in NMR, mass spectrometry, and X-ray crystallography. Dr. Trempe contributed greatly to this project by performing X-ray crystallography data collection and mass spectrometry. I would like to thank Dr. Guennadi Kozlov for his expertise in NMR spectroscopy and NMR experiments that allowed me to analyze the data obtained.

I would like to thank my Research Advisory Committee members, Dr. Heidi McBride and Dr. Lawrence Kazak for their valuable advice during my research. Moreover, I would like to acknowledge Jean Luo, Cordelia Cho, and Zhidian Zhang for being supportive friends and colleagues. I am eternally grateful for their continuous support and stimulating discussions. Finally, I would like to thank my Mom, Dad, and my little sister for always being there for me.

I am thankful to the McGill Faculty of Medicine internal studentship and the Healthy Brain and Healthy Lives fellowship for the funding provided for my project.

Author Contribution

The majority of the results of this thesis have been published as part of a manuscript for Nature Structural and Molecular Biology (Sauvé, V., Sung, G., Soya, N., Kozlov, G., Blaimschein, N., Miotto, L. S., Trempe, J.-F., Lukacs, G. L., & Gehring, K. (2018)).

I expressed and purified the constructs for the UbcH7-parkin fusion, performed sortase A reactions, screened crystallization conditions, refined the crystal structure, performed pUb-UbVS assay, and wrote and edited the manuscript.

Dr. Véronique Sauvé designed constructs for the UbcH7-parkin fusion, froze crystals, performed autoubiquitination assays, prepared HDX samples, screen crystallization conditions, refined the crystal structure, and wrote and edited the manuscript.

Dr. Naoto Soya and Dr. Gergely Lukacs performed HDX experiments and analysis.

Dr. Lis Schwartz Miotto and Nina Blaimschein expressed and purified samples for NMR experiments.

Dr. Guennadi Kozlov performed the NMR experiments.

Dr. Jean-François Trempe collected X-ray data, performed phasing and crystal structure refinement, analyzed E2:parkin interactions, and wrote and edited the manuscript.

and Dr. Kalle Gehring wrote and oversaw the project.

List of Abbreviations

ATP – Adenosine triphosphate

Bd or BD – *Bactrocera dorsalis*

CLS – Canadian Light source

CMCF - Canadian Macromolecular Crystallography Facility

DTT - Dithiothreitol

GBA - glucocerebrosidase

GST – Glutathione S-transferase

HDX-MS – Hydrogen-Deuterium Exchange Mass Spectrometry

HECT – Homologous to the E6-AP carboxyl terminus

HEPES – 4-(2-hydroxyethyl)-1-piperazineethanesulfonic acid

Hs or HS – *Homo sapiens*

IBR – In-Between-RING domain

LB – Luria Broth

MDV – Mitochondria-derived vesicle

MitAP – Mitochondrial antigen presentation

PD – Parkinson's Disease

PDB – Protein data bank

PEG – Polyethylene glycol

PINK1 – PTEN-induced putative kinase 1

pUb – phosphorylated ubiquitin

Rn or RN – *Rattus norvegicus*

REP – Repressor element of parkin

RBR - RING-between-RING

RING – Really interesting new gene

SAD – Single wavelength anomalous diffraction

SDS-PAGE – Sodium dodecyl sulphate polyacrylamide gel electrophoresis

STING – stimulator of interferon gene

Snx9 – Sorting nexin 9

SUMO – Small ubiquitin-like modifier

Tc or TC - Tribolium castaneum

TCEP - tris(2-carboxyethyl) phosphine

Tris-tris (hydroxymethyl) aminomethane

Ubl – Ubiquitin-like domain

UHPLC – Ultra-high performance liquid chromatography

Ulp1 – Ubiquitin-like-specific protease 1

WT – Wild-type

XDS – X-ray detection software

List of Figures

Figure 1: Different ubiquitin chains generated by various RBR E3 ligases17
Figure 2: The topology of zinc fingers of each RING and RING-like domain in RBR E3 ligases.
Figure 3: Domain organization of parkin
Figure 4: Sequence alignments of parkin orthologs and E2 enzymes
Figure 5: Typical purification profile for obtaining UbcH7-pParkin for crystallization
Figure 6: Autoubiquitination assay and crystal structures of phosphorylated <i>Bactrocera</i> parkin
fused to UbcH7, in the presence of pUb
Figure 7. Structure of ternary complex of activated parkin
Figure 8. Highlights of activated parkin structure
Figure 9: Steric interactions regulate parkin activity
Figure 10: Electrostatic interactions between UbcH7 and parkin RING1
Figure 11: Ubiquitination assay of activated parkin and GST-parkin
Figure 12: pUbl binding site verified by NMR experiment
Figure 13: Sortase A ligation of ¹⁵ N-Ubl and ¹⁴ N-R0RBR
Figure 14: Complementary assay resolving conflicting model
Figure 15. HDX-MS detection of conformational changes upon activation of rat parkin by
phosphorylation and phospho-ubiquitin binding
Figure 16. NMR experiment of different amount of pUb
Figure 17: pUb activation of Parkin through RING052
Figure 18. Pathway of parkin activation. 53
List of Tables
Table 1: Data collection and refinement statistics

1. Introduction

1.1 Parkinson's Disease (PD)

In 1817, James Parkinson first described the symptoms later used as distinguishing features of Parkinson's Disease (PD) in his essay, *An Essay on the Shaking Palsy* (James Parkinson, 2002). In his essay, Parkinson defined Shaking Palsy as "involuntary tremulous motion, with lessened muscular power, in parts not in action and even when supported; with a propensity to bend forwards, and to pass from a walking to a running pace: the senses and intellects being un-injured" (James Parkinson, 2002). Later, in 1872, Jean-Martin Charcot termed "Parkinson's Disease" after James Parkinson. Moreover, one of Charcot's major contribution to PD as a disease was the differentiation of Parkinson's from other tremorous disorders such as multiple sclerosis (Goetz, 2011). In 1912, Frederick Heinrich Lewy first discovered intraneural inclusions, which was later termed Lewy bodies by Konstantin Nikolaevich Tretiakoff in 1919 (Lewy, 1912; Trétiakoff, 1919; Engelhardt et al., 2017). Moreover, Tretiakoff reported the presence of Lewy bodies in the *substantia nigra*, which contains dopaminergic neurons that supplies dopamine to the striatum (Trétiakoff, 1919).

These studies became the foundation for our knowledge in PD and allow the development of many different therapies. In his essay, Parkinson advocated for early therapeutic intervention when presented, such as blood-letting, followed by induced blistering near the cervical vertebrae (James Parkinson, 2002). On the other hand, Charcot used hyoscyamine, which is anticholinergic, as well as rye-based products, which are the pharmacological basis of some modern dopamine agonists. Charcot later advocated for vibratory therapy after observing a reduction of resting tremors in patients who had taken carriage rides (Charcot, 1892). In the mid-twentieth century, a wide variety of anticholinergic drugs were developed, but they displayed similar efficacy and side

effect profiles (Onuaguluchi, 1968). Efforts in finding effective drugs lead to the discoveries of dopamine-based drugs such as L-dopa and its precursor levodopa (Birkmayer et al., 1961; Barbeau, 1969; Cotzias et al., 1969; Yahr et al., 1969).

Parkinson's Disease (PD) is the second common neurodegenerative disease characterized by motor symptoms that are largely caused by the loss of dopaminergic neurons in the *substantia nigra*. The documented symptoms of PD include both motor and psychological. Most patients exhibit motor symptoms that might include tremors, muscle rigidity, and difficulty with walking. However, some will also exhibit psychological symptoms such as dementia, depression, anxiety. Most cases of PD occur sporadically in older people, and about 15% of the PD cases have a family history of the disease (Deng et al., 2018). However, about 5-10% of the PD patients suffer the monogenic form of the disease that follows Mendelian inheritance pattern (Deng et al., 2018). These autosomal mutations allowed researchers to narrow into the pathology of PD. So far, there are three pathways identified that cause the pathogenesis of PD. The first is the inability to clear away insoluble Lewy Bodies, the second is the inability to properly clear away damaged mitochondria, and the last is the inflammatory response upon the formation of the mitochondria-derived vesicle (MDV) and the presentation mitochondrial.

1.2 Pathology of PD

The first pathology of PD is the formation of Lewy bodies, which is neuronal inclusion bodies, in the brain. α -synuclein is the most common protein found in the Lewy Bodies, and mutations in α -synuclein are the second most common type of the dominant form of PD (Shults, 2006). α -synuclein is a protein that is involved in lipid membrane interaction and vesicle trafficking (DeWitt et al., 2013). Moreover, mutations in α -synuclein have been shown to lead to

its aggregation; however, other gene mutations, such as LRRK2, can also cause aggregation of α -synuclein (Miklossy et al., 2006; Lin et al., 2009). In the case of non-mutated α -synuclein, post-translational modifications, such as phosphorylation and nitrosylation, may lead to its aggregation (Anderson et al., 2006; Liu et al., 2011). Furthermore, mutation in another protein, glucocerebrosidase (GBA), is found to be associated with Lewy body disorder. GBA is the most common genetic risk factor for PD and has been associated with sporadic PD (Sidransky et al., 2012; Baden et al., 2019).

The second type of PD pathology is characterized by the inability to deal with mitochondria dysfunction. In familial PDs, mutations are categorized into dominant forms and recessive forms. The most common cause of dominant PD is the mutations in Leucine-rich Repeat Kinase 2 (LRRK2) (Funayama et al., 2002). LRRK2 is a large (280 kDa) multidomain protein that has two distinct enzymatic domains: the kinase domain for phosphorylation and the ROC-GTPase domain for GTP-GDP hydrolysis (Greggio et al., 2008). LRRK2 has been found to be involved in various cellular functions and signaling pathways (Rideout et al., 2014). The most common mutation is found in the kinase domain, which increases the LRRK2 kinase activity (Greggio et al., 2008). Moreover, LRRK2 has been found to interact with numerous regulators of mitochondrial fission/fusion (Wang et al., 2012; Stafa et al., 2013), but how mutant LRRK2 leads to mitochondrial dysfunction is still unclear. However, it has been shown that LRRK2 is also involved in Rab signaling and cellular trafficking pathways in neurons (Purlyte et al., 2018; Marte et al., 2019).

The most well-known proteins that are involved in mitochondrial quality control are the *PARK2* (parkin) (Kitada et al., 1998) and *PARK6* (PTEN-induced putative kinase 1 (PINK1)) (Valente et al., 2004) genes. Mutations in parkin and PINK1 are responsible for the recessive form

of early-onset of Parkinson's disease. Parkin, an E3-ubiquitin ligase, and PINK1, a mitochondrial ser/thr kinase, constitute a mitochondrial quality control system that controls autophagy (mitophagy) of depolarized and defective mitochondria (Pickles et al., 2018). Loss of function mutations in these two genes results in an early onset of PD.

Recently, it has been found that the immune response is responsible for the progression of PD. The formation of mitochondria-derived vesicle (MDV) and the presentation of mitochondrial antigen (MitAP) has been linked to auto-immune response (Matheoud et al., 2016; Matheoud et al., 2019). Since autophagy plays a role in immune tolerance, it was thought that MitAP is a result of mitophagy; however, this process is driven by the MDVs formation. For both MitAP and MDV formation, Sorting nexin 9 (Snx9), responsible for clathrin-mediated endocytosis, is required (Shin et al., 2007; Matheoud et al., 2016). Furthermore, Rab9, a late endosomal/Golgi GTPase, is recruited to mitochondrial for the MDV formation, while Rab7 is recruited for the fusion of MDVs with endosomal compartments (Kucera et al., 2016). The presence of MitAP leads to the autoimmune attack on the neurons, and MitAP is inhibited mainly by PINK1 and parkin (Matheoud et al., 2016). In addition, Snx9 is degraded in the presence of parkin, suggesting a new substrate for parkin that is not involved in the mitophagy pathway (Matheoud et al., 2016). Aside from MDV/MitAP-dependent immune response, parkin and PINK1 have been shown to be involved in STING-mediated inflammation, which can result from mitophagy (Sliter et al., 2018). Parkin and PINK1 play an important role in mitochondrial quality control and immune response.

1.3 Ubiquitination Pathway

Protein turnover is an essential cellular process that allows non-functional proteins to be degraded and new ones to be made (Komander et al., 2012). One of the most prevalent degradation

pathways is the protein ubiquitination pathway (Komander et al., 2012; Swatek et al., 2016). Protein ubiquitination is a key post-translational modification that is involved in the regulation of cellular proteins which are signaled for degradation (Komander et al., 2012). The ubiquitin degradation pathway occurs via three steps; ubiquitin activation, conjugation, and the ligation of ubiquitin to the substrate (Komander et al., 2012). The ubiquitin is first activated by E1 activation enzyme (E1) in an ATP-dependent manner (Dove et al., 2016). Ubiquitin is then transferred to E2 conjugating enzyme (E2) through trans-thioesterification (Dove et al., 2016). The E2 enzyme catalyzes the transfer of ubiquitin to either the E3 ligases (E3) or the substrate depending on the type of E3 ligases used in the reaction (Ye et al., 2009). All of these enzymes accomplish the transfer of ubiquitin through thioester bonds (Dove et al., 2016); however, in the last step of the pathway, an isopeptide bond is formed between the substrate and ubiquitin (Dove et al., 2016).

Ubiquitination can occur as long as there is lysine available, generating multiple ubiquitination sites (Komander et al., 2012). Ubiquitination usually occurs on a lysine residue of the substrate but can also occur on the N-terminus or more rarely on serine and threonine residues. Moreover, ubiquitin can be added to other ubiquitin to generate ubiquitin chains because ubiquitin has seven lysines (Komander et al., 2012). Different types of polyubiquitination chains lead to different signaling pathways and these often lead to protein degradation (Figure 1) (Komander et al., 2012). For example, linear chains, which are generated by the HOIP/HOIL-1L complex or Linear Ubiquitin Assembly Complex (LUBAC), signal for the NF-kB pathway during an immune response (Komander et al., 2012). In addition, K63 polyubiquitination often signals for DNA repair and lysosomal degradation (Komander et al., 2012), whereas the K48 polyubiquitination signals for proteasomal or lysosomal degradation (Chau et al., 1989; Komander et al., 2012).

It has been previously suggested that Parkin is able to form branched ubiquitin chains such as the formation of Lys 63, Lys 48, and Lys 27 branched polyubiquitin chains (Cunningham et al., 2015). Recently, it was discovered that Parkin has a preference to form Lys 6 chains, although its signaling pathway is poorly understood (Cunningham et al., 2015). Structurally, the crucial residue that has been implicated to aid the transfer of ubiquitin is the histidine residue that is two residues away from the catalytic cysteine (Trempe et al., 2013). Although the preference for a certain type of chain has been discovered, the mechanisms in which they are transferred are still unclear.

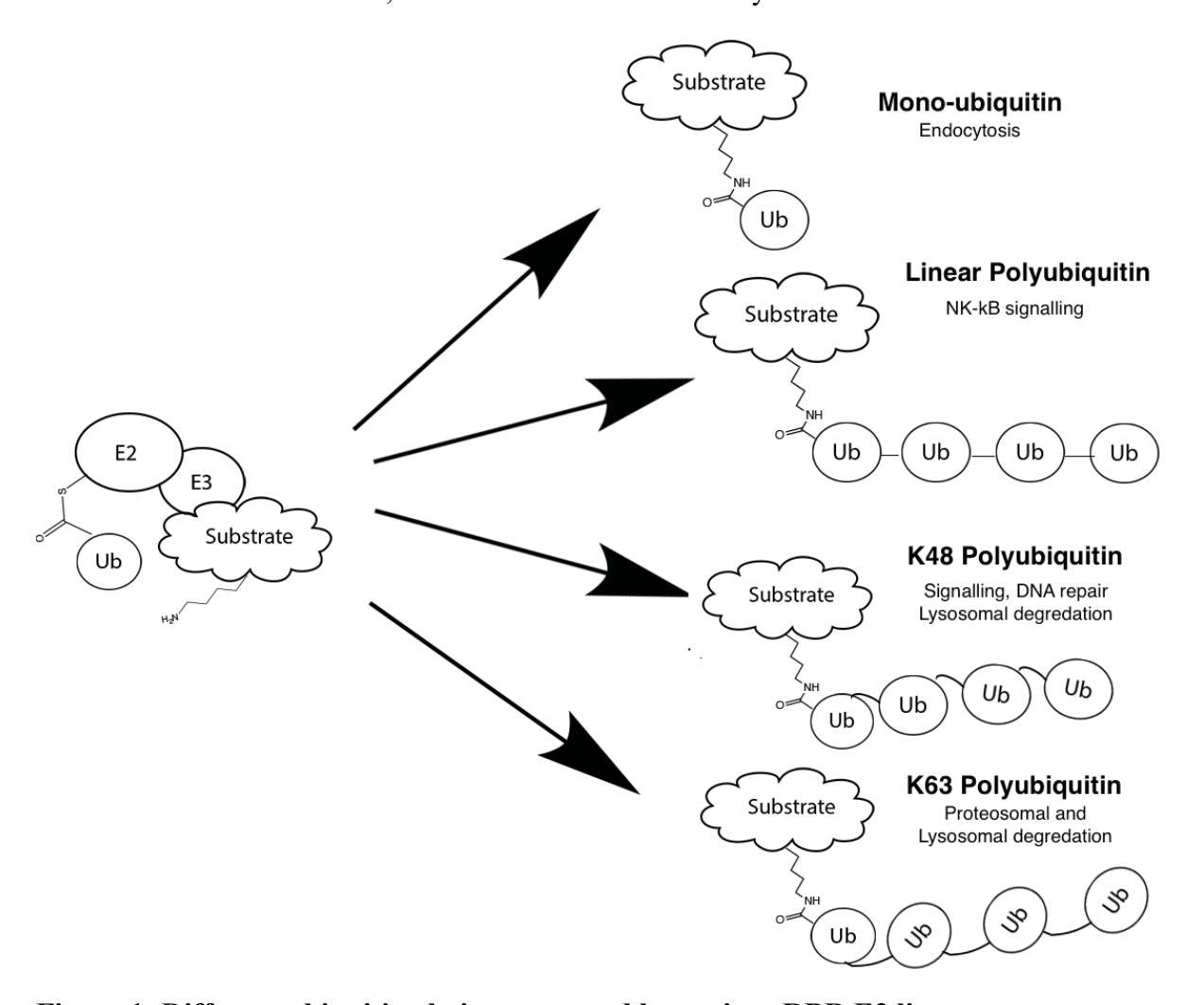


Figure 1: Different ubiquitin chains generated by various RBR E3 ligases. The different ubiquitin chains shown have many different signaling pathways. Linear chains can be generated by the LUBAC system by HOIP/HOIL-1L, K63 and K48 chains can be generated by either Parkin or the Ariadne Family.

1.4 Types of Ubiquitin E3 ligases

In humans, there are many different types of E3 ligases, and they are categorized based on their domain architecture and their ubiquitin transfer mechanisms. There are three main types of E3 ligases. The first type is the RING (Really Interesting New Gene) type ligase, which binds 2 Zn²⁺ ions and allows direct transfer of ubiquitin to the substrate directly (Berndsen et al., 2014). The second type of E3 is the HECT (Homologous to the E6AP Carboxyl Terminus) type ligase, which the ubiquitin is first transferred to, and then to the substrate (Berndsen et al., 2014). The third type of ligase is the RBR (RING-Between-RING) E3 ligases which contain Zn²⁺-binding RING domains but perform the HECT-type ubiquitin transfer mechanisms (Berndsen et al., 2014). Although these E3 ligases participate in the ubiquitination pathway, other accessory domains among these enzymes give rise to their own unique forms of regulation in the cell.

1.5 RBR E3 ligases

RBR E3 ligases have three characteristic Zn²⁺-binding domains known as the RING1, inbetween Ring (IBR), and RING 2 domains. In all of these domains, the coordination with Zn²⁺ ions occurs through seven cysteines and one histidine (Trempe et al., 2013). The RING1 domain is structurally similar and exhibits the same function for the binding of E2 enzyme as the RING domains of RING type E3 ligases (Trempe et al., 2013). The RING1 domain is important for the binding of E2 enzyme, as this domain is highly conserved among the RBR E3 ligases in terms of structure (Trempe et al., 2013). The RING1 domain displays the characteristic cross-brace motif structure observed in RING ligases (Figure 2) (Trempe et al., 2013). The RING2 domain in the RBR ligases, despite bearing the same name, is not a true RING domain. It is not able to bind to E2 conjugating enzymes and has a different structure (Smit et al., 2014). In the RBR E3 ligases,

the transfer of ubiquitin is done between the E2 enzyme and the RING2 domain through transthioesterification (Dove et al., 2016). The role of the IBR domain remains unclear. The IBR domain is required for function but displays flexibility in known structures (Sauvé et al., 2015; Trempe et al., 2013).

Although RBR E3 ligases all have the same core domains, different domains within each ligase provide different regulatory functions. For example, parkin activity is inhibited by its Ubl (ubiquitin-like) domain and a unique RING0 domain and the Repressed Element of Parkin (REP) linker (Trempe et al., 2013). In addition, HOIP and HOIL-1L, another group of E3 ligases, form a complex to carry out polyubiquitination reactions (Spratt et al., 2014). HOIP is modulated by Ubiquitin Associated (UBA) domain, which is involved in autoinhibition; however, the binding site for the UBA domain on HOIP is still unknown (Lechtenberg et al., 2016). Like Parkin, HOIL-1L contains a Ubl domain; however, it acts as a trans-activating agent for the HOIP ligase instead of an autoinhibitory domain (Sato et al., 2011). In addition, both HOIP and HOIL-1L contain NZF domains that are involved in the stabilization of linear ubiquitin chains (Sato et al., 2011). Another class of RBR E3 ligases is the Ariadne family, which has a signature Ariadne domain at their Cterminus (Smit et al., 2014). The Ariadne domain in the HHARI ligase has been shown to interact with its RING2 domain, similarly to the RING0 domain on Parkin, to produce its own autoinhibition (Duda et al., 2013). Despite having completely different structures, both Ariadne and RING0 domains restrict the access to the catalytic cysteine (Duda et al., 2013; Trempe et al., 2013).

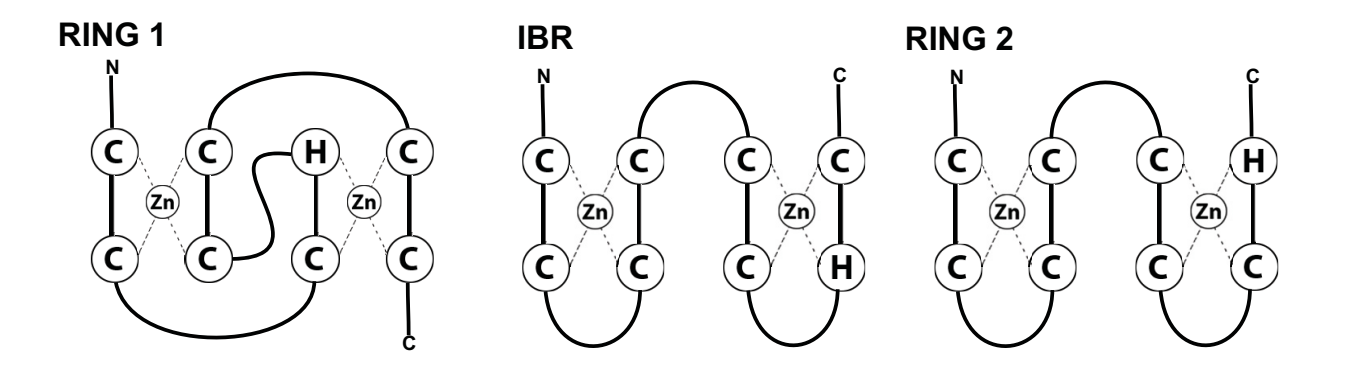


Figure 2: The topology of zinc fingers of each RING and RING-like domain in RBR E3 ligases.

The RING1 domain displays a topology that is characteristic of the RING domain in RING-type E3 ligases. The IBR and RING2 domains shown similar topology. Upon studying the structure coordinate for various E3 ligases, the fold observed for the RING1 domain of Parkin is similar across the RBR E3 ligases. Figure adapted from (Trempe et al. 2013).

As mentioned before, the RBR E3 ligases all contain a RING1 domain, which is involved in the binding of the E2 conjugating enzyme (Dove et al., 2016). There are many E2s that have the ability to bind different E3s, and some E2s have the ability to either use the RING-type transfer mechanism or HECT-type mechanism (Ye et al., 2009). Moreover, the discovery of UbcH7 (E2) that could not transfer ubiquitin directly to a lysine residue indicated that the RBR E3 ligases behaved like HECT-type ligases (Wenzel et al., 2011). However, since RBR E3s behave like the HECT-type and use the RING1 domain to bind to E2s, there are E2s that can interact with both types (Ye et al., 2009). Some of the most common types of E2s that have been shown to interact with most RBR E3s are UbcH7 and UBCH5b (Wenzel et al., 2011). These E2s have been shown to have some preference for the types of ubiquitin chains it makes, but it has been demonstrated that E2s might not be as specific as we previously thought. For example, it has been documented that E2s such as Ube2K, which normally produces Lys 48 chains, produces a linear chain in conjunction with the HOIP/HOIL-1L complex (Chen et al., 1991; Kirisako et al., 2006; Smit et al.,

2012). Generally, it is suggested that the E2 might influence the type of ubiquitin chains they make, but the HECT and RBR E3 ligases should presumably dictate the types of ubiquitin chains made.

1.6 Parkin as an RBR E3 Ligase

Parkin is a cytosolic E3 ubiquitin ligase consisting of an N-terminal ubiquitin-like (Ubl) domain connected by a long linker to four consecutive Zn²⁺ binding domains: RING0, RING1, IBR, and RING2 (Figure 3). Parkin is basally autoinhibited but becomes activated to induce mitophagy (Trempe et al., 2013; Wauer et al., 2013; Riley et al., 2013).

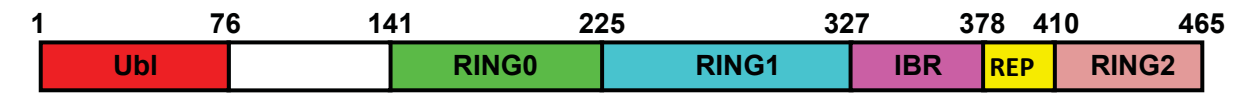


Figure 3: Domain organization of parkin.

Parkin consists of an N-terminal ubiquitin-like (Ubl) domain connected by a long linker to four consecutive Zn²⁺ binding domains: RING0, RING1, IBR, and RING2. Between IBR and RING2 is the REP linker. Figure adapted from Trempe et al. 2013

The process is initiated by the accumulation of PINK1, a serine/threonine protein kinase on the mitochondrial outer membrane (Geisler et al., 2010; Matsuda et al., 2010; Narendra et al., 2010; Vives-Bauza et al., 2010). PINK1 phosphorylates nearby ubiquitin molecules to trigger parkin recruitment through its affinity for phosphorylated ubiquitin (pUb) (Kane et al., 2014; Kazlauskaite et al., 2014; Koyano et al., 2014; Ordureau et al., 2014). This allows PINK1 to phosphorylate parkin on its Ubl domain, which activates its ubiquitination activity (Sauvé et al., 2015; Kazlauskaite et al., 2015; Wauer et al., 2015; Kumar et al., 2015). The generation of newly attached ubiquitin molecules on mitochondria that can be phosphorylated by PINK1 generates a positive feedback mechanism for the recruitment of more parkin (Ordureau et al., 2014). Ubiquitination of mitochondrial proteins by parkin leads to the recruitment of mitophagy receptors (Pickles et al., 2018). Parkin and PINK1 have also been implicated in autophagy-independent

processes such as the production of MDV carrying damaged cargo (Sugiura et al., 2014) and suppression of MitAP (Matheoud et al., 2016).

1.7 Parkin activation

Parkin activity requires the transfer of ubiquitin from E2 onto its active cysteine before being transferred onto a substrate (Wenzel et al., 2011). Like other RBR E3 ligases, parkin has an E2 binding site on its RING1 domain and a catalytic RING2 domain (Seirafi et al., 2015). Parkin activity is controlled by autoinhibitory elements. The Ubl domain and the REP linker sterically hinder the E2 binding site on RING1 domain while the catalytic site is occluded by RING0 (Trempe et al., 2013; Wauer et al., 2013; Riley et al., 2013; Kumar et al., 2015). In the REP linker, tryptophan 403 (W403) is involved in the binding of RING1 domain. Mutations on W403 have been associated with higher Parkin activity because the hydrophobic residue fits in the RING1 domain (Trempe et al., 2013). Aside from the E2 binding site, parkin has another regulation site located at the RING2 -RING0 interface (Trempe et al., 2013). The active cysteine (C431) required for the trans-thiolation is buried between the hydrophobic interfaces of the RING2 and RING0 domain (Trempe et al., 2013). Therefore, activation of parkin would require an additional conformational change to bring the RING2 and E2 active sites together for ubiquitin transfer. Binding of pUb increases parkin activity slightly, but crystal structures of parkin-pUb only showed local rearrangements within the RING1 domain and a shift of the IBR domain (Wauer et al., 2015; Kumar et al., 2017).

1.8 Research objective

Up until recently, the only known structures of Parkin were autoinhibited structures. Through the overlay of the autoinhibited structures of Parkin and E2-bound RING-type E3 ligase, we observed three problems. The first problem is that the Ubl domain and the REP linker occludes the binding site for E2 enzyme. The second problem is the active cysteine on RING2 is buried between the hydrophobic interface between RING2 and RING0. The last problem is the distance between the active cysteine of E2 and RING2 is 50Å apart. Because of these issues, we hypothesized that there will be a major conformational change when Parkin is phosphorylated. In 2015, various groups have shown that pUb can activate parkin, so many attempts to crystallize parkin in the presence of pUb were carried out. However, even with the presence of pUb, there were no significant conformational changes that indicate parkin activity.

This thesis describes the structure of phosphorylated parkin in complex-pUb and the E2 enzyme UbcH7. The structure reveals that phosphorylation of the parkin Ubl domain leads to a large conformational change that releases both inhibitory interactions and allows the parkin and E2 catalytic sites to come together. While the RING2 domain is not visible in our crystal structure, we can infer changes in its position from measurements of its solvent exposure in hydrogen-deuterium exchange (HDX) experiments. The results provide a complete picture of the activation of parkin through binding of pUb and parkin phosphorylation. Moreover, since pUb and pUbl share 32% identity, we hypothesized that there is a possibility that pUb and pUbl could both activate parkin when it is recruited to the mitochondria. This regulation was first observed in our NMR experiments and verified using Ub-Vinyl Sulfone (UbVS) assay, which allows us to measure the degree of RING2 release.

2. Material and Methods

2.1 Primer Used

Primer 1: 5'-teggatetggaagttetgttecaggggeeetgggatecatggeggeeageaggaggetg-3'

Primer 2: 5'-gecacegeggatececeaagtacaggttttcacegeggtecacaggtegettttccc-3'

Primer 3: 5'-gaggeteacagagaacagattggtggcggtggcggtgcgaaaccgacctaccactetttettcg-3'

Primer 4: 5'-gtggtggtggtggtggtgctcgagtgcgcactaaacgtcgaaccagtggtcacccatgcacgc-3'

2.2 Construct Used

Parkin:

GST-Bactrocera Parkin

GST-Rat Parkin

GST-Rat Parkin (K161N)

GST-Rat Parkin (R163N)

GST-Rat Parkin (K211N)

GST-rat parkin (1-86)-LPETGG

His-SUMO-GGG-rat parkin (141-465)

GST-Human Parkin

GST-Human Parkin (K211N)

UbcH7-Parkin Fusion:

GST-UbcH7(C86K)-10aa linker-Δ1-29 & Δ117-160 *B. dorsalis* parkin (C463A)

GST-UbcH7(C86K)-10aa linker-Δ1-29, Δ117-160 & Δ412-496 B. dorsalis parkin (C463A)

Ubiquitin:

Ubiquitin from bovine erythrocytes (Sigma-Aldrich: U6253)

Ubiquitin Vinyl Sulfone (UbVS)

His-SUMO-Ubiquitin (S65A)

Other enzymes:

His-mouse E1

GST-TcPINK1(143-570)

His-sortase A enzyme

2.3 Cloning, expression, and purification of recombinant proteins in E. coli

Gibson assembly (NEB) was used to generate fusion proteins with GST-tag followed by human UbcH7 and fruit fly parkin. A PCR fragment containing the UbcH7 gene was amplified using Primer 1 and Primer 2 with pET28a-LIC-UbcH7 vector as template. *Bactrocera dorsalis* parkin DNA without the sequence coding for 29 amino acids at the N-terminus and codonoptimised for E. coli expression was synthesized by Bio Basic Inc. and subcloned into the BamHI-XhoI sites of pGEX-6P1 (GE Healthcare). The GST-UbcH7-Bactrocera parkin fusion was made by ligating the UbcH7 gene with a 13 amino acid linker between GST and *Bactrocera* parkin through BamHI restriction site. Single-point mutations and segment or domain deletions were performed using PCR mutagenesis (Agilent). Constructs expressing GST-UbcH7(C86K)-10aa linker-Δ1-29 & Δ117-160 *Bactrocera* parkin (C463A) and GST-UbcH7(C86K)-10aa linker-Δ1-29, Δ117-160 & Δ412-496 *Bactrocera* parkin (C463A) proteins were used for the production of the crystallized proteins.

The construct for the expression of the acyl donor, GST-rat parkin (1-86)-LPETGG, for the sortase A reaction was created by PCR mutagenesis by introducing six amino acids LPETGG and a stop codon after the Ubl domain of the pGEX-rat parkin vector. The construct for the expression of acyl acceptor, His-SUMO-GGG-rat parkin (141-465), was cloned using the Gibson assembly method. The PCR fragment, amplified using Primer 3 and Primer 4 and pGEX-rat parkin as template, was assembled in the BamHI-HindIII fragment of the pSmt3 vector.

Protein expression was conducted in BL21 (DE3) *E. coli*. UbcH7-parkin fusion, full-length and parkin deletions, were expressed with 500 uM ZnCl₂ and 25 uM IPTG. UbcH7 and Tc-PINK1 were expressed with 500 uM IPTG. GST-tagged proteins were purified by glutathione-Sepharose (GE Healthcare) followed by 3C precision protease cleavage to remove GST tag, then size-exclusion chromatography. His-tagged proteins were purified by Ni-NTA agarose (Qiagen) affinity and size-exclusion chromatography. His-SUMO-tagged proteins were purified by Ni-NTA agarose (Qiagen) affinity followed by Ulp1 protease cleavage, then size-exclusion chromatography. ¹⁵N-labeled Ubl and Ub were produced in M9 minimal medium supplemented with ¹⁵NH₄Cl. Sortase A expression was performed in Rosetta 2 *E. coli* induced with 500 μM IPTG at 25°C. Sortase A was purified using Ni-NTA affinity followed by size exclusion chromatography. Purified proteins were verified using Tris-glycine SDS-PAGE analysis. Protein concentrations were determined using UV absorbance.

2.4 Phosphorylation of parkin complex and ubiquitin

33 μM of UbcH7-parkin was phosphorylated with 100 μM of bovine ubiquitin (Sigma), 1μM GST-TcPINK1(143–570), 50 mM Tris–HCl pH 8.0, 150 mM NaCl, 1 mM TCEP-HCl, 10 mM MgCl₂, and 5 mM ATP at 30°C for 2 hours. The complex was purified by size-exclusion

chromatography. The phosphorylation of the complex was verified using a 7.5 % Tris-glycine gel containing 20 µM Phos-tag (ApexBio) and 40 µM MnCl₂ and stained with Coomassie blue.

To obtain large amounts of phosphorylated Ubl or Ub, 100 uM of Ubl or Ub was phosphorylated in the presence of 3 uM of PINK1, 50 mM Tris pH 7.4, 150 mM NaCl, 5 mM ATP, and 10 mM MgCl₂. The reaction was conducted at 30°C for 2 hours, and the reaction was then subjected to size-exclusion chromatography for pUbl and monoQ for pUb. Ion exchange of pUb was performed using a linear gradient from 20 mM Tris pH 8.7 to 50 mM Tris pH 7.4.

2.5 Autoubiquitination assays of rat parkin

The autoubiquitination assays of WT and mutant rat parkin were done in two steps: first, the proteins were phosphorylated by TcPINK1 in the presence of ubiquitin, then the autoubiquitination reaction was carried. The phosphorylation step was performed at 30 °C for 2.5 hours in 50 mM Tris pH 7.4, 150 mM NaCl, 0.5 mM TCEP, 4 mM ATP, 8 mM MgCl₂ with 0.1 μM GST-Tc-PINK1, 10 μM ubiquitin (Sigma) and 3 μM parkin. An aliquot was taken to analyze the level of phosphorylation of the proteins using mass spectrometry or Phos-tag SDS-PAGE analysis. Autoubiquitination reactions were performed at 37 °C for 30 min for parkin samples or 20 min for GST-parkin samples, by adding 50 nM mouse His-E1, 3 μM UbcH7, 40 μM ubiquitin, 2 mM ATP and 5 mM MgCl₂ to 2.25 uM of phosphorylated parkin. The same protocol was used for the autoubiquitination assays of UbcH7-Bactrocera parkin fusion, except that the addition of UbcH7 was omitted. Complementation assays of parkin mutants used 1 or 2 μM phosphorylated parkin in the presence of 0 or 3 μM UbcH7, 50 nM E1, 50 μM ubiquitin and 100 nM TcPINK1. Reactions were stopped by the addition of 5× SDS-PAGE loading buffer, and the level of

ubiquitination was analyzed on 10% Tris-glycine gels stained with Coomassie blue. All assays were performed once (n=1).

2.6 Crystallization

Initial crystals of the UbcH7-phosphorylated Bactrocera parkin-pUb complex were grown using hanging drop vapor diffusion method by mixing protein at 1 μl of protein complex at 4.6 mg/ml in 10 mM Tris-HCl pH 8.0, 5 mM NaCl, 1 mM TCEP with 1 μl of 0.1 M HEPES pH 6.5, 6% isopropanol, 50 mM MgCl₂ and 5% (w/v) PEG 4K at 4 °C. Those microcrystals were diluted and used as seeds to set up hanging drops including 1.5 μl of protein complex at 4.6 mg/ml, 1 μl of reservoir solution and 0.5 μl of seed solution. Crystals appeared after 3-4 days. After 2 weeks, crystals were cryoprotected in mother liquor supplemented with 25% (v/v) glycerol before being cryo-cooled in liquid nitrogen.

Crystals of the UbcH7-phosphorylated Bactrocera parkinΔR2- pUb complex were grown using hanging drop vapor diffusion method by mixing 1 μl of protein complex (4.7 mg/ml) in 10 mM Tris-HCl pH 8.0, 5 mM NaCl, 1 mM TCEP with 1 μl of 0.1 M Tris-HCl pH 8.0, 15% (w/v) PEG 2K MME and 0.1 M KCl at 4°C. Crystals appeared after 2-3 days. After 6 days, crystals were cryoprotected in mother liquor supplemented with 22.5% (v/v) glycerol before being cryo-cooled in liquid nitrogen.

2.7 Data collection and structure determination

Diffraction data for both proteins were collected at the CMCF beamline 08ID-1 at the Canadian Light Source. For the UbcH7-phosphorylated parkin-pUb complex, a total of 330 images were collected with an oscillation angle of 0.5° at the Zn K-edge (1.283 Å). Reflections were

integrated and scaled using the XDS package (Kabsch, 2010). The structure was solved using a combination of molecular replacement and SAD using Phaser and AutoSol implemented in the PHENIX packages (Adams et al., 2010; McCoy et al., 2007; Afonine et al., 2012; Terwilliger et al., 2009). The diffraction data were first phased by molecular replacement using RING1-IBR-pUb (from PDB deposition 5CAW) as a search model. Further molecular replacement allowed the positioning of UbcH7 molecule (from PDB 5UDH). The analysis of the Zn anomalous signal allowed us to determine six sites in the asymmetric unit. Four sites confirmed the correct positioning of RING1 and IBR domains. The remaining two Zn sites allowed us to position the RING0 domain (from PDB 5CAW). The unassigned density next to RING0 was fitted with the Ubl domain (from PDB 4ZYN). No electronic density could accommodate the RING2 domain.

For the UbcH7-phosphorylated parkinΔR2-pUb complex, a total of 270 images were collected with an oscillation angle of 0.5° at 1.033Å. Reflections were integrated and scaled using the XDS package (Kabsch, 2010). The structure was solved by molecular replacement using the previously determined complex structure as a search model. Refinements were done using the PHENIX package (Adams et al., 2010) and the model buildings were performed using COOT (Emsley et al., 2010). Calculated Ramachandran values for the final structures of UbcH7-phosphorylated parkin-pUb and UbcH7-phosphorylated parkinΔR2-pUb complexes are, respectively, 94% and 93% of residues in the favored region, and 1 and 0 outliers.

2.8 Sortase A reactions

15 μ M of acyl acceptor (GGG- Δ Ubl-parkin) was mixed with 50 μ M of acyl donor (GST-Ubl-LPETG) in 50 mM Tris pH 8.0, 200 mM NaCl, 10 mM CaCl₂, and 1 mM DTT with 5 μ M of sortase A enzyme. The reaction was dialyzed overnight at 4 °C. The product was purified with

GST affinity chromatography. After GST affinity chromatography, the GST tag was removed with 3C precision protease followed by size exclusion chromatography.

2.9 NMR experiments

Rat parkin was used for NMR studies. ¹⁵N-labeled pUbl, ¹⁵N-Ubl-¹⁴N-parkin (141-465) (segmentally labeled parkin) and unlabeled parkin (141-465) constructs were buffer-exchanged into NMR buffer (20 mM Tris-HCl, 120 mM NaCl, 2 mM DTT, pH 7.4). All parkin-pUb complexes were purified by size-exclusion chromatography in NMR buffer. Titrations were performed by adding unlabeled parkin proteins to 60 μM ¹⁵N-pUbl proteins in excess (1:2 molar ratio) to form the complex. For ¹⁵N-Ubl-¹⁴N-parkin WT and K211N mutant, the individual spectrum was collected at 60 μM. 60 μM pUb was added to segmentally labeled parkin (1:1 molar ratio), and spectra were collected. The segmentally labeled parkin-pUb complex was phosphorylated with GST-TcPINK1 in the presence of MgCl₂ and ATP. GST-TcPINK1 was removed with GST-affinity beads, and the spectrum of segmentally labeled phosphorylated parkin-pUb was measured again. ¹H-¹⁵N correlation spectra were acquired at 25 °C for the segmentally labeled parkin and 5 °C for the ¹⁵N-labeled pUbl titrations at field strengths of 600 MHz and 800 MHz using Bruker spectrometers equipped with a triple-resonance (¹H, ¹³C, ¹⁵N) cryoprobe. Spectra were processed using NMRpipe and analyzed with SPARKY (Delaglio et al., 1995).

2.10 Hydrogen-deuterium exchange mass spectrometry (HDX-MS)

Rat parkin was used for HDX-MS studies. HDX samples were first verified by intact mass spectrometry (Impact II Q-TOF, Bruker). HDX was initiated by diluting 120-160 µM stock solution of parkin or parkin-pUb complex using 1:14 dilution ratio into the D₂O-based buffer. The

HDX incubation period and temperature were set to 10, 60, 300, 900 s and 30 °C. The exchange was quenched with chilled buffer (300 mM glycine, 8 M urea in H₂O, pH 2.4) using 2:13 dilution ratio. Quenched samples were flash frozen in a dry ice methanol bath and stored at –80 °C until use. For the undeuterated control, initial dilution was made in H₂O buffer.

Prior to ultra-high performance liquid chromatography (UHPLC)-MS analysis, the deuterated parkin was digested in an on-line immobilized pepsin column prepared in house. Resulting peptides were loaded onto a C₁₈ analytical column (1-mm inner diameter, 50 mm length; Thermo Fisher Scientific) equipped to an Agilent 1290 Infinity II UHPLC system. Peptides for each sample were separated using a 5–40% linear gradient of acetonitrile containing 0.1% formic acid for 8 min at a 65 µl/min flow rate. To minimize back-exchange, the columns, solvent delivery lines, injector, and other accessories were placed in an ice bath. The C₁₈ column was directly connected to the electrospray ionization source of the LTQ Orbitrap XL (Thermo Fisher Scientific), and mass spectra of peptides were acquired in the positive-ion mode for m/z 200–2000. Duplicate measurements were performed for each time point. Identification of peptides was carried out in separate experiments by tandem MS (MS/MS) analysis in data-dependent acquisition mode, using collision-induced dissociation. All MS/MS spectra were analyzed using Proteome Discoverer 1.4 (Thermo Fisher Scientific). Peptide searching results were further manually inspected, and only those verifiable were used in HDX analysis. Percent deuteration as a function of incubation time was determined using HDExaminer 2.3 (Sierra Analytics, Modesto, CA) and presented in Supplementary Data Set 3. The first two amino acid residues in peptides were excluded from the analysis (Bai et al., 1993). The standard deviation in deuteration across technical repeats (n=3) was approximately 1%.

2.11 UbVS assay

Different amounts of pUb or pUbl were first added to 5 µM of R0RBR/pUb (WT or K211N) complex. 10 uM of UbVS (Boston Biochem) was then added to the mixture in 25 mM Tris pH 8.5, 200 mM NaCl, 5 mM TCEP. The reaction was performed at 37°C for a total time of 90 minutes; time points were taken at 15, 45, and 90 minutes. Reactions were stopped by the addition of 5× SDS-PAGE loading buffer with DTT (40 mM), and the level of ubiquitination was analyzed on 10% Tris-glycine gels stained with Coomassie blue. All assays were performed once (n=1).

2.12 Data Availability

The atomic coordinates and structure factors of the activated parkin crystal structures were deposited in the Protein Data Bank under accession codes 6DJW and 6DJX. Source data for Figure 7 are available with the paper online. Other data are available from the corresponding author upon reasonable request.

3. Results

3.1 Crystallization of activated parkin

In order to learn how parkin is activated after phosphorylation, I screened a large variety of conditions and protein constructs of UbcH7-parkin fusions to obtain protein crystals of activated parkin. Although we have screened a variety of the fusions with different species of parkin, the best crystals were obtained with parkin from Bactrocera dorsalis, an oriental fruit fly. The protein is 43% identical to human parkin (Figure 4). To favor co-crystallization with the E2 enzyme, we employed a fusion protein consisting of human UbcH7 followed by parkin. This approach has been employed for crystallization of other E2-RING complexes (McGinty et al., 2014). Bactrocera parkin contains an N-terminal extension in front of the Ubl, which was deleted, and the Ubl-RING0 linker was shortened. The fusion protein was purified described in Materials and methods (Figure 5). After obtaining the pure protein, UbcH7-Parkin with different length linkers were phosphorylated by PINK1 in the presence of Ub, and crystallization screens were set up in the presence of pUb. The fusion protein was able to catalyze the steps of ubiquitin transfer in *in vitro* assays (Figure 6a). We obtained crystals that diffracted to 4.8 Å resolution and were able to solve the structure using molecular replacement and analysis of the Zn anomalous signal (Table 1; Figure 6b). No electron density or Zn anomalous signals were observed for REP linker and RING2 domain despite their presence in the crystallized protein. As the crystal lattice contains large voids between protein molecules, we interpreted the missing density as an indication that the domains are disordered.

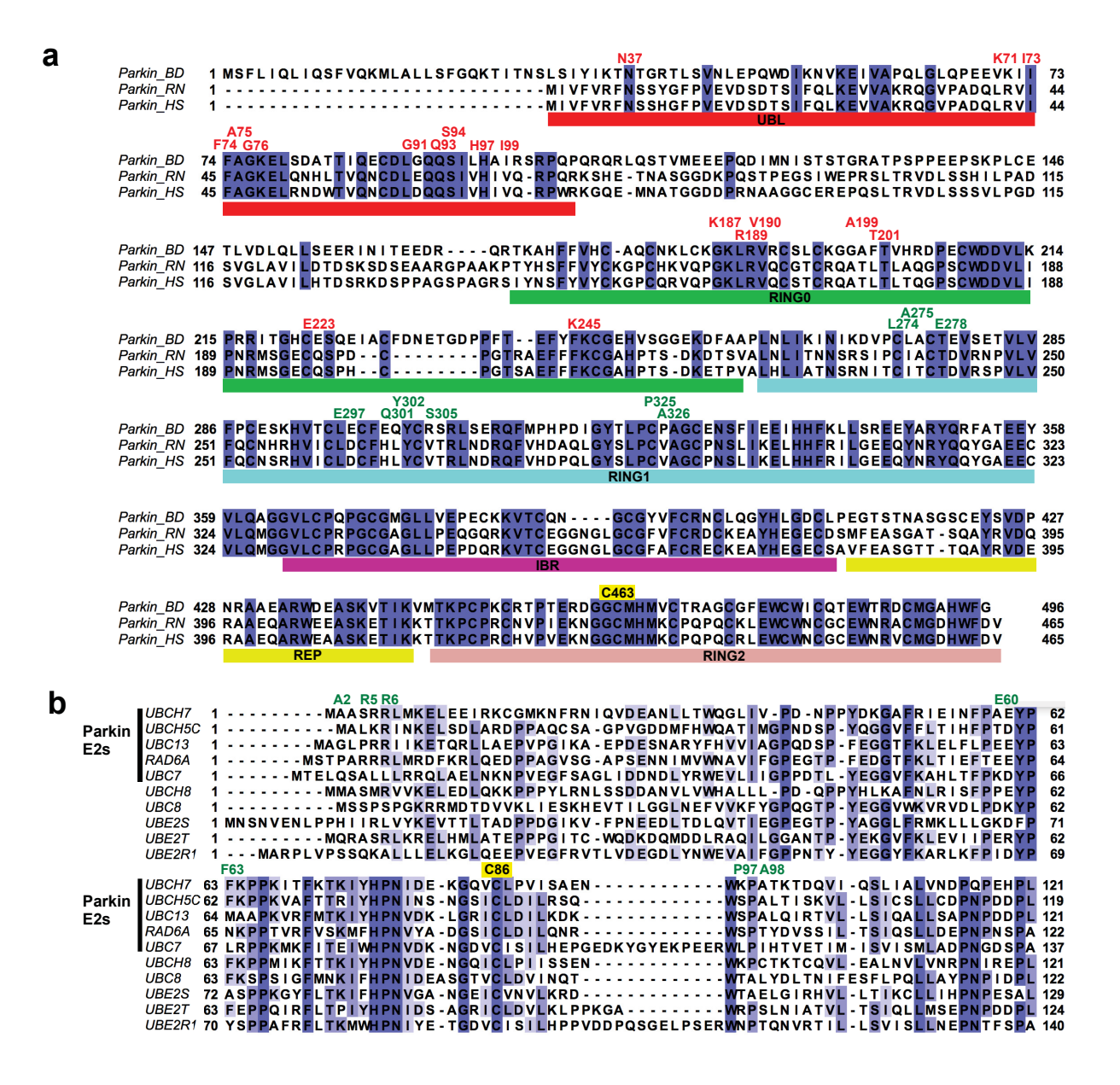


Figure 4: Sequence alignments of parkin orthologs and E2 enzymes.

a, Sequence alignment of parkin orthologs from *Bactrocera dorsalis* (BD), *Rattus norvegicus* (RN) and *Homo sapiens* (HS). **b**, Sequence alignment of human E2 ubiquitin-conjugating enzymes. The first five E2 enzymes have been reported to function with parkin *in vitro* or in cells. Blue shading indicates sequence conservation. Residues in the parkin-UbcH7 interface are labeled in green. Residues in the pUbl-RING0 interface are labeled in red. The catalytic cysteines are labeled in yellow.

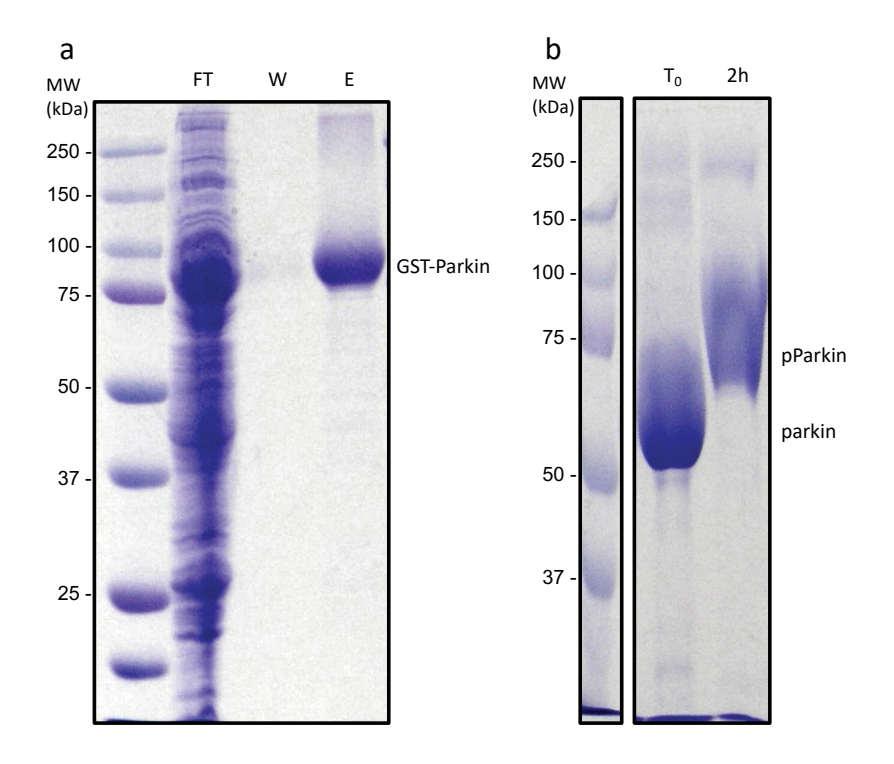


Figure 5: Typical purification profile for obtaining UbcH7-pParkin for crystallization. a, GST purification of UbcH7-parkin where FT stands for flow-through, W stands for wash, and E stands for elution. The purification was visualized on 10% SDS-PAGE. b, Phosphorylation of UbcH7-parkin in the presence of ubiquitin where T_0 is time zero and 2h is two hours. The reaction was stopped by adding 5X-SDS loading buffer and was visualized on 7.5% phos-tag SDS-PAGE (n=1).

Table 1: Data collection and refinement statistics

	UbcH7-phosphorylated parkin	UbcH7-phosphorylated parkin
	Δ RING2 + pUb	+ pUb
	(PDB 6DJW)	(PDB 6DJX)
Data collection	(122 020)	(' '
Space group	P3 ₁ 21	P3 ₁ 21
Cell dimensions		
a, b, c (Å)	134.6, 134.6, 86.2	135.6, 135.6, 88.0
α, β, γ (°)	90, 90, 120	90, 90, 120
Resolution (Å)	48.28-3.80 (3.94-3.80) ^a	48.84-4.80 (4.97-4.80) ^a
$R_{ m merge}$	0.096 (2.31)	0.078 (0.62)
$I/\sigma(I)$	15.0 (1.2)	17.3 (4.3)
$CC_{1/2}$	0.999 (0.406)	0.999 (0.879)
Completeness (%)	100.0 (100.0)	100.0 (100.0)
Redundancy	9.8 (9.9)	9.7 (10.1)
Refinement		
Resolution (Å)	3.8	4.8
No. reflections	9,146 (908)	4,778 (465)
$R_{ m work}$ / $R_{ m free}$	0.26 /0.30	0.26/0.29
No. atoms		
Protein	4,340 (550 aa)	4,340 (550 aa)
Zinc	6	6
B factors		
Protein	215	300
Zinc	223	312
R.m.s. deviations		
Bond lengths	0.005	0.003
(Å)		
Bond angles (°)	0.80	0.75

Single crystals were used for structure determination. ^aValues in parentheses are for the highest-resolution shell.

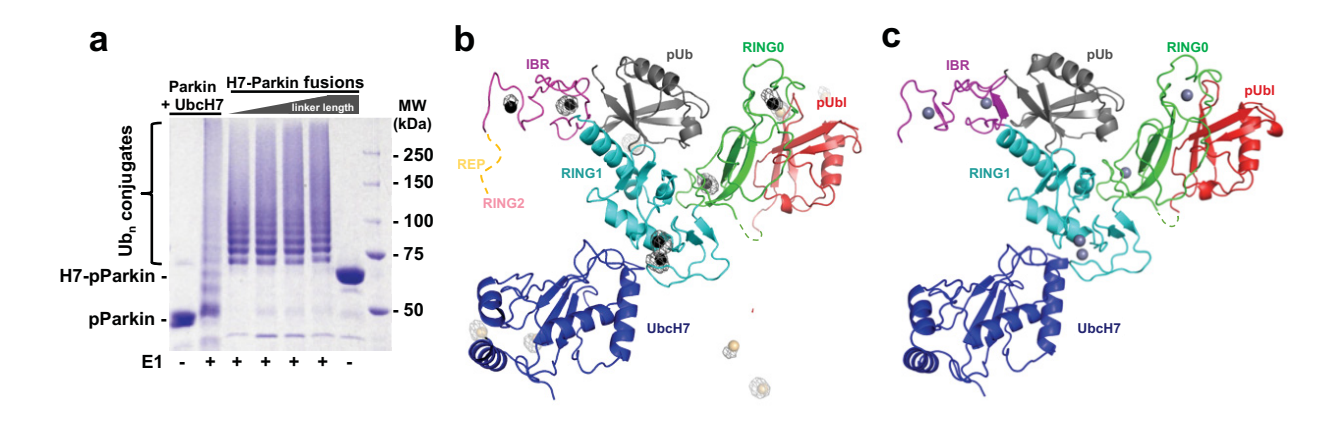


Figure 6: Autoubiquitination assay and crystal structures of phosphorylated *Bactrocera* parkin fused to UbcH7, in the presence of pUb.

a, The autoubiquitination activity of UbcH7-parkin fusion protein was tested with phosphorylated proteins in the presence of Ub and visualized on SDS-PAGE gel (*n*=1). The first two lanes show the activity of UbcH7 and parkin alone as a control. The third to sixth lanes show the activity of the UbcH7-parkin fusions with different length linkers. The linker length between UbcH7 and parkin is 8, 10, 13, 15 amino acids. **b**, The structure with the REP linker and RING2 present was solved to 4.8 Å using molecular replacement and zinc SAD. The anomalous map was generated from data collected for UbcH7-phosphorylated parkin/pUb crystal at 1.28 Å wavelength. The anomalous dispersion (*light grey mesh*) confirms the position of zinc atoms (*black spheres*) of RING0 (*green*), RING1 (*cyan*) and IBR (*magenta*) in the crystal structure of UbcH7-phosphorylated parkin/pUb. Zinc atoms of symmetry-related UbcH7-phosphorylated parkin/pUb molecules within the crystal are displayed in light orange. No unassigned anomalous density was observed. **c**, The structure without the disordered elements was solved to 3.8 Å using molecular replacement using 4.8 Å structure as the model. The all-atom root mean square deviation between the two structures is 0.2 Å.

In the second round of crystallization trials, I deleted the REP linker and RING2 domain from the fusion protein (Figure 7a). Since parkin in its inactive conformation is poorly soluble without the RING2 domain, the truncated protein was co-expressed in *E. coli* with PINK1 and ubiquitin. The ternary complex of active parkin was purified and yielded improved crystals that diffracted to 3.8 Å (Table 1, Figure 6c). The structure solved from the second set of crystals was essentially identical to the first (Figure 6c). Removal of the flexible REP-RING2 segment had no structural impact on the rest of the protein complex but significantly improved the quality of the crystals. No density was observed for the UbcH7-parkin linker, and when we calculated the distance between the N-terminus of parkin and C-termini of UbcH7 in our current structure, the

distance is greater than 10 amino acids in the UbcH7-parkin linker. Therefore, we infer that the UbcH7-parkin interface arises from distinct polypeptide chains in the crystals (Figure 7c).

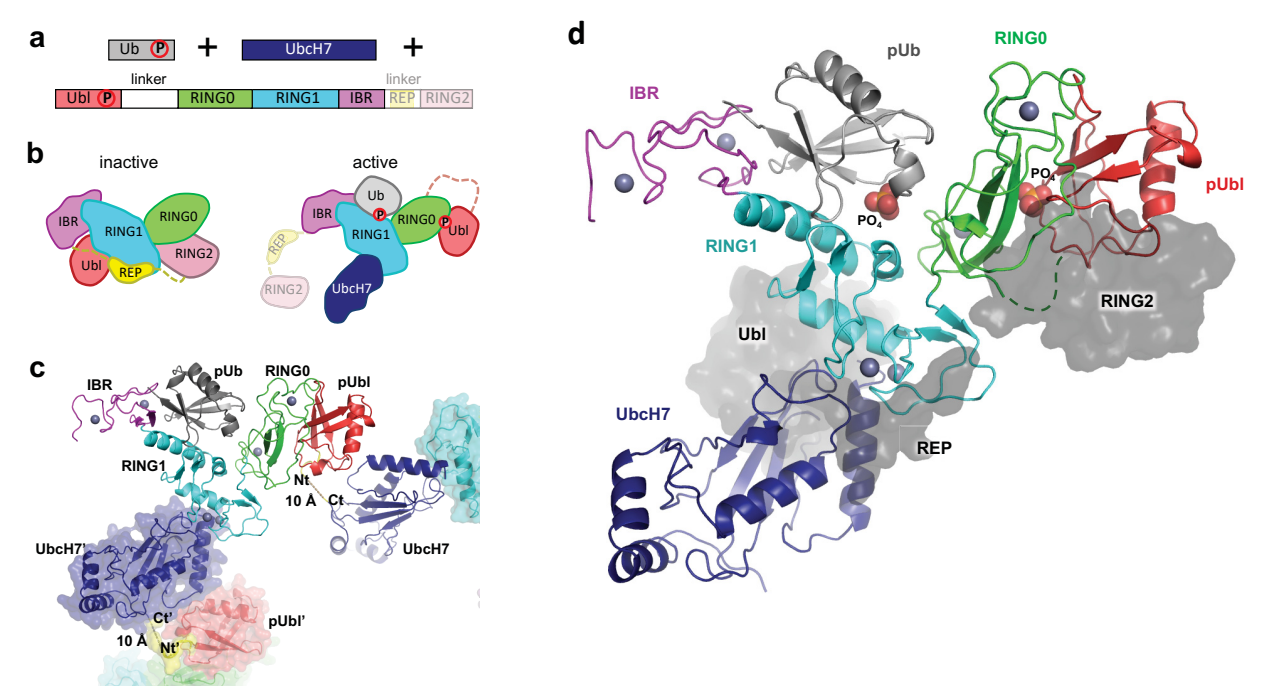


Figure 7. Structure of ternary complex of activated parkin.

a, Domain organization of proteins in the complex: phosphorylated ubiquitin (pUb), E2 enzyme UbcH7, and phosphorylated parkin. The REP linker and RING2 were disordered or absent in the crystals. Parkin and ubiquitin are phosphorylated. **b**, Schematic of parkin domain rearrangements. **c**, Polypeptide connectivity in the crystal. From the distance between the visible electron density of the C-terminus of UbcH7 (Ct) and the N-terminus of the Ubl domain (Nt), we infer that UbcH7 and parkin from different polypeptides come together to generate the UbcH7-RING1 interface. This linkage is a consequence of crystal packing and the length of the linker and does not represent a relevant biological assembly. **d**, Crystal structure of the ternary complex. The overlaid Ubl, REP linker, and RING2 domains from the inactive parkin (PDB 4K95, *grey surface*) show the large domain movements upon activation.

3.2 Structural analysis of activated parkin

The protein structures reveal major rearrangements associated with parkin phosphorylation and pUb and E2 binding (Figure 7b,d). In agreement with previous studies, (Wauer et al., 2015; Kumar et al., 2017; Sauvé et al., 2015; Kumar et al., 2015), we observed pUb bound primarily to the RING1 domain with additional contacts to the RING0 and IBR domains. pUb binding results

in a 50° shift of the IBR domain up and away from the E2 (Figure 8a). Because the pUb C-terminus was chemically cross-linked to the IBR domain in the previous structures, it was unknown how much of the structural rearrangement was due to the cross-link (Wauer et al., 2015; Kumar et al., 2017; Gladkova et al., 2018). However, we see identical changes including the existence of an intermolecular parallel β-sheet between the pUb C-terminus and the IBR domain (Figure 8a). Recognition of the phosphoserine is mediated by a binding site consisting of two positively charged residues and a tyrosine on RING1. This site is conserved across species with the substitution of Lys340 by arginine in human parkin (Figure 8b). The large number of contacts is responsible for the nanomolar binding affinity and strong selectivity for pUb.

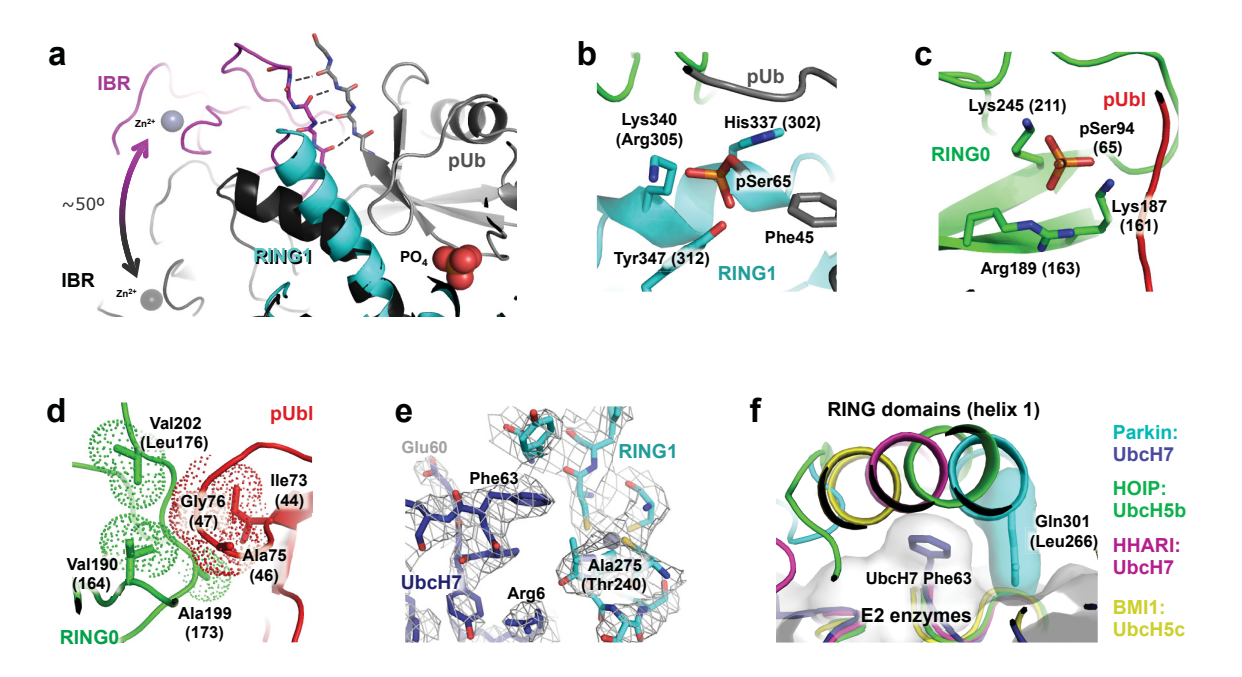


Figure 8. Highlights of activated parkin structure.

a, Overlay of inactive (*black*) and active conformations shows that pUb binding leads to straightening of an α-helix in RING1 and a large upward shift of the IBR domain. The C-terminus of pUb forms a short β-sheet with a strand from the IBR domain. b, Detail of the pUb phosphate-binding site on RING1. c, Detail of the pUbl phosphate-binding site on RING0. d, RING0:pUbl interface showing hydrophobic contacts. e, Refined $2F_o$ - F_c electron density map (B-factor sharpened) at the UbcH7:RING1 interface shows contacts around parkin Ala275, equivalent to human Thr240 which is mutated in PD (Sauvé et al., 2015; Shimura et al., 2000). f, Overlay of the structures of RBR RING:E2 complexes (this work, PDB 5EDV, PDB 5UDH, PDB 3RPG), shows the variable position of the RING helix. Residue labels in parentheses indicate numbering in human parkin.

Activation of parkin induces a large shift in the position of the Ubl domain. The domain is bound to RING1 in autoinhibited parkin, but upon phosphorylation, it moves to RING0 (Figure 6d). In this conformation, the E2-binding site on RING1 becomes available, whereas the RING2 cannot bind to RING0 because of overlap with pUbl (Figure 9a). The pUbl phosphoserine is stabilized by positively charged residues, two lysines and an arginine (Figure 8c). This site was one of two sulfate binding sites observed in inactive parkin crystal structures (Sauvé et al., 2015; Wauer et al., 2013; Swatek et al., 2016). Additional contacts are mediated by the Ubl hydrophobic patch (corresponding to Ile44 of ubiquitin) and a loop centered around a conserved Ubl glycine, which inserts into a hydrophobic groove in RING0 (Figure 8d). While this paper was under review, the structure of truncated, human parkin phosphorylated on serine 65 cross-linked to pUb was published (Gladkova et al., 2018). That structure shows the same shift of the Ubl domain upon phosphorylation as well as additional contacts from a conserved region of the Ubl-RING0 linker.

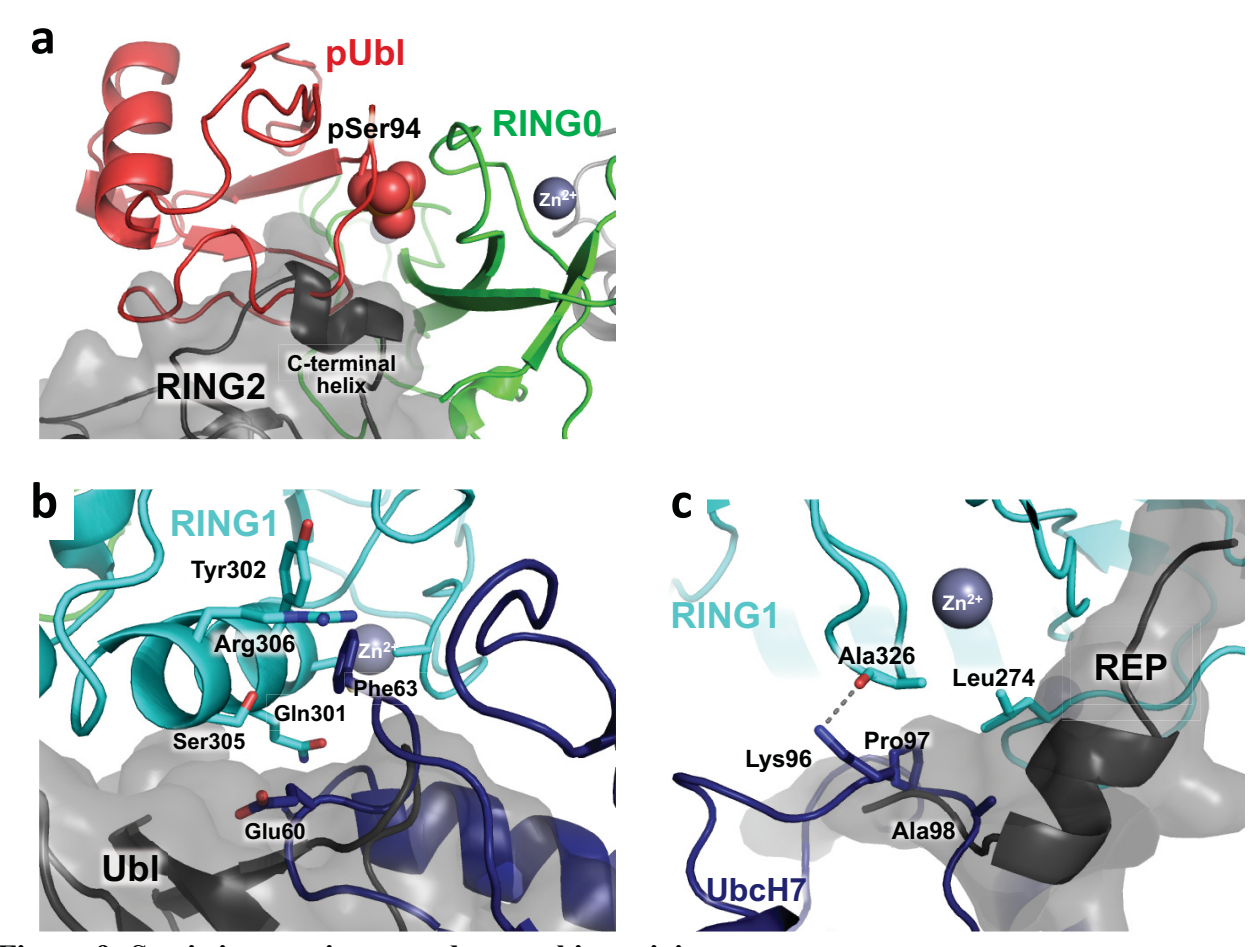


Figure 9: Steric interactions regulate parkin activity

a, Overlay of activated *Bactrocera* parkin structure (*colored*) with the RING2 modeled from the inactive parkin (*grey*, PDB 4K95). The C-terminal helix of RING2 occupies the same position as pUbl residues preceding the phosphoserine residue (pSer94). **b**, Overlay of UbcH7 with the Ubl domain from inactive parkin. The Ubl domain prevents UbcH7 residues Glu60 and Phe63 from binding to residues Gln301, Tyr302, Ser305, and Arg 306 of helix 1 of the parkin RING1 domain. **c**, Overlay of UbcH7 with the REP linker from inactive parkin. The REP residues preceding the helix block contact of UbcH7 residues Lys96, Pro97, and Ala98 with *Bactrocera* parkin residues Ala326 and Leu274

UbcH7 binds RING1 at the conserved E2-RING interaction site (Figure 6d). RING1 is the only parkin domain with similarity to E2-binding domains of other RING E3 ligases (Trempe et al., 2013; Wauer et al., 2013; Riley et al., 2013; Spratt et al., 2013). The N-terminus and loops 4, and 7 of UbcH7 interact with helix 1 and a zinc-coordination site of RING1. Phe63 of loop 4 of UbcH7 interacts with Ala275 (Thr240 and Ala240 in human and rat parkin, respectively) (Figure 8e). Mutation of the residue to arginine is a PD mutation and disrupts UbcH7 binding (Sauvé et

al., 2015; Hattori et al., 1998; Shimura et al., 2000). Another mutation at this site, T240M, has also been reported in several autosomal recessive PD families (Periquet et al., 2003). Superposition of RING:E2 structures via the strongly conserved E2 domains shows that helix 1 in RING1 adopts a different position relative to other RING domains (Figure 8f). This allows Gln301 (Leu266 in human and rat) to contact UbcH7 via van der Waals interactions; consistently, Kumar and colleagues reported that the L266K mutation in human Parkin, which would cause steric clashes with the E2 enzyme, reduces GST-Miro ubiquitination (Kumar et al., 2015). The side-chains of Arg5 and Arg6 in the N-terminal helix of UbcH7 mediate electrostatic interactions with an acidic patch that is conserved in parkin RING1 (Figure 10). These two basic residues are conserved in E2 enzymes that have been reported to function with parkin (Figure 9b).

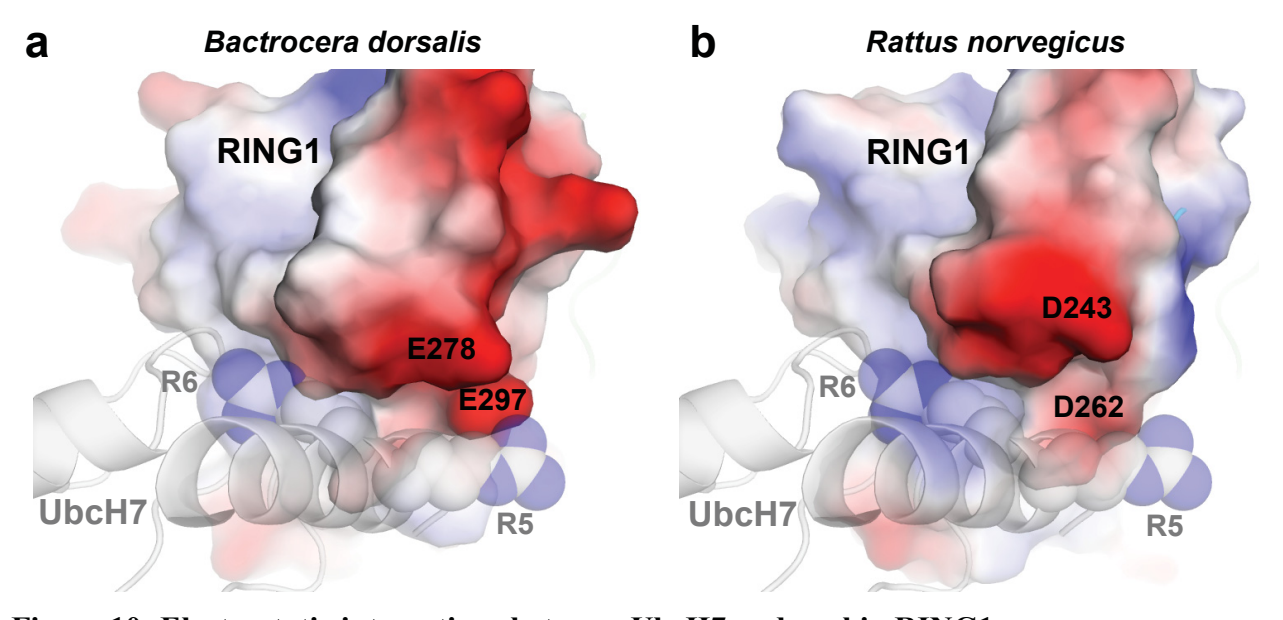


Figure 10: Electrostatic interactions between UbcH7 and parkin RING1

a, Structure of *Bactrocera* parkin bound to UbcH7. An electrostatic potential map was calculated for the isolated RING1 domain. The side-chains of Arg5 and Arg6 in UbcH7 interact with a negatively charged surface in RING1. **b**, Model of rat Parkin (PDB 4ZYN) bound to UbcH7 with an electrostatic potential map computed for the isolated RING1 domain (REP and Ubl removed).

The structure also explains the inability of the inhibited conformation of parkin to bind E2 enzymes; the RING1 helix 1 is inaccessible due to the bound Ubl domain (Figure 9b). Mutations

in this helix that repel the Ubl promote parkin activation (Sauvé et al., 2015; Kumar et al., 2015; Tang et al., 2017). Similarly, the REP linker in the inactive parkin blocks contacts between the parkin zinc-coordination site and loop around the highly conserved proline 97 in UbcH7 (Figure 9c).

3.3 Ubl phosphorylation is important for activation

To assess the importance of the protein-protein contacts observed in our crystal structure and rule out artifacts related to the use of the Bactrocera protein or E2-parkin fusion, we conducted validation experiments with rat parkin. Autoubiquitination assays were used to test the importance of the pUbl-binding site for parkin activity. The basic residues, Lys161, Arg163, and Lys211, were individually mutated to asparagine and the mutant proteins phosphorylated by PINK1. Phos-tag SDS-PAGE confirmed the mutants were all fully phosphorylated (Figure 11a). Autoubiquitination assays with both GST-tagged and untagged parkin proteins showed a dramatic loss of activity for the three mutants (Figure 11b,c). While N-terminal tags have been reported to activate parkin (Chaugule et al., 2011), in our assay, the addition of the GST-tag to the parkin N-terminus did not diminish the ligase activity. The K161N mutant showed some residual activity, but the R163N and K211N were completely inactive. This corroborates previous studies that showed these mutants are impaired in recruitment to the mitochondria (Geisler et al., 2010; Matsuda et al., 2010; Narendra et al., 2010), MDV production (McLelland et al., 2014), activation, and ubiquitin chain assembly (Ordureau et al., 2014). These results highlight the importance of the integrity of this RING0 site for parkin activity and explain why missense mutations of Lys161 and Lys211 are disease mutations (Abbas et al., 1999; Pankratz et al., 2009).

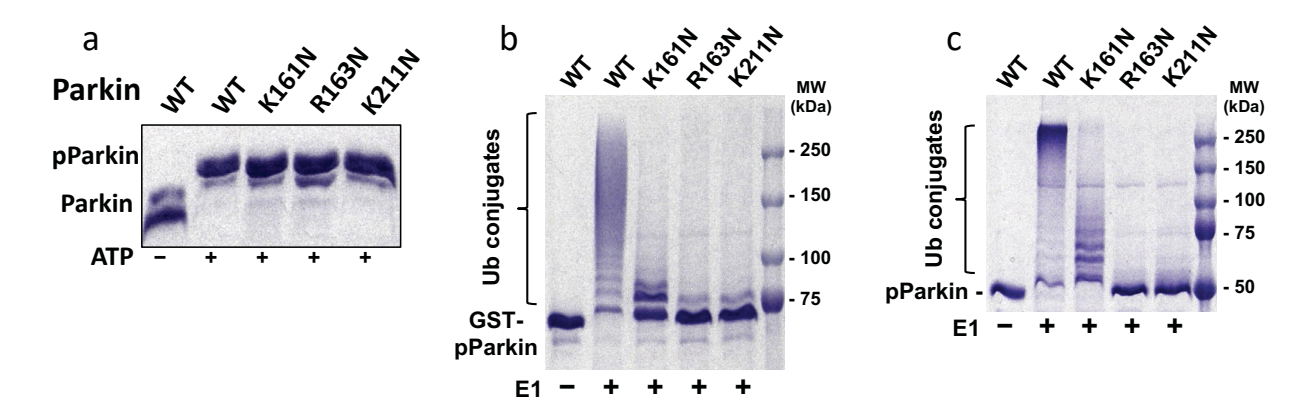


Figure 11: Ubiquitination assay of activated parkin and GST-parkin a, For the autoubiquitination assay, the mutants and WT were phosphorylated and verified on a 7.5% phos-tag SDS-PAGE. b,c, SDS-PAGE gels showing that pUbl binding site mutants of rat GST-parkin (GST-pParkin) and pParkin are defective in autoubiquitination.

NMR experiments were performed to confirm that RING0 binds pUbl. The parkin Ubl domain gives excellent ¹⁵N-¹H correlation spectra, which have been fully assigned (Safadi et al., 2007; Aguirre et al., 2017). Addition of parkin without the Ubl domain (ΔUbl-parkin) to ¹⁵N-labeled pUbl led to the progressive weakening of several signals and the complete loss of the signal from phosphorylated Ser65. This signal loss is due to exchange broadening from pUbl binding to ΔUbl-parkin. In contrast, the addition of the K211N mutant had no effect on the phosphorylated Ser65 signal indicating no binding occurred (Figure 12a). The relatively small changes in the pUbl spectrum upon addition of wild-type parkin reflect the low affinity of the intermolecular interaction.

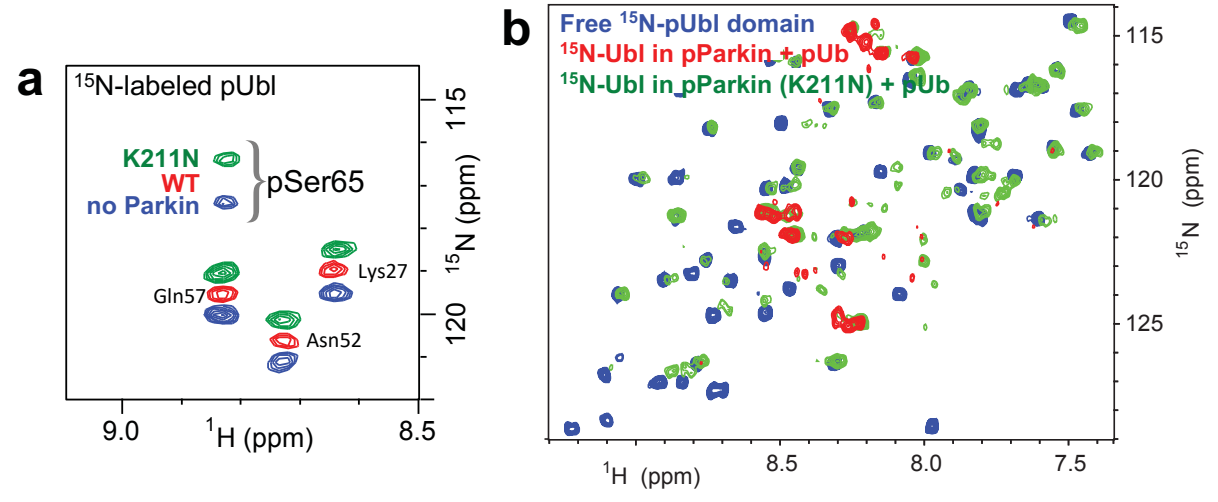


Figure 12: pUbl binding site verified by NMR experiment

a, Comparison of spectra of the isolated ¹⁵N-labeled pUbl domain in the absence and presence of Δ Ubl-parkin and pUb. The spectra were shifted for comparison. pUbl binding to parkin results in loss of the amide signal from phosphoserine 65 (pSer65). No binding was observed with the Δ Ubl-parkin K211N mutant. **b**, NMR spectra of the free phosphorylated Ubl domain (*blue*) and full-length parkin specifically ¹⁵N-labeled on the Ubl domain. Few signals are observed in the spectrum of wild-type parkin (*red*) due to intramolecular binding of the pUbl domain to RING0. Mutation of the pUbl-binding site releases the pUbl domain and yields a spectrum (*green*) similar to that of the free pUbl domain.

To look at pUbl binding in a more physiological context, we used the sortase A protein ligation system (Steffen et al., 2016) to generate a parkin protein in which only the Ubl domain (residues 1-85) was ¹⁵N-labeled. The sortase A protein ligation system is a technique to ligate two segments of peptides by using the sortase A enzyme. The sortase A will recognize the signal peptide sequence of LPXTGG on the C-terminus of the first fragment and ligate it to the second fragment with a poly-glycine N-terminus (Theile et al., 2013). The Ubl domain and R0RBR were purified separately, and they were ligated together using the sortase A protein (Figure 13a). The purity of the segmentally labeled parkin was verified on an SDS-PAGE (Figure 13b,c). After verification, we then carried out our NMR experiment.

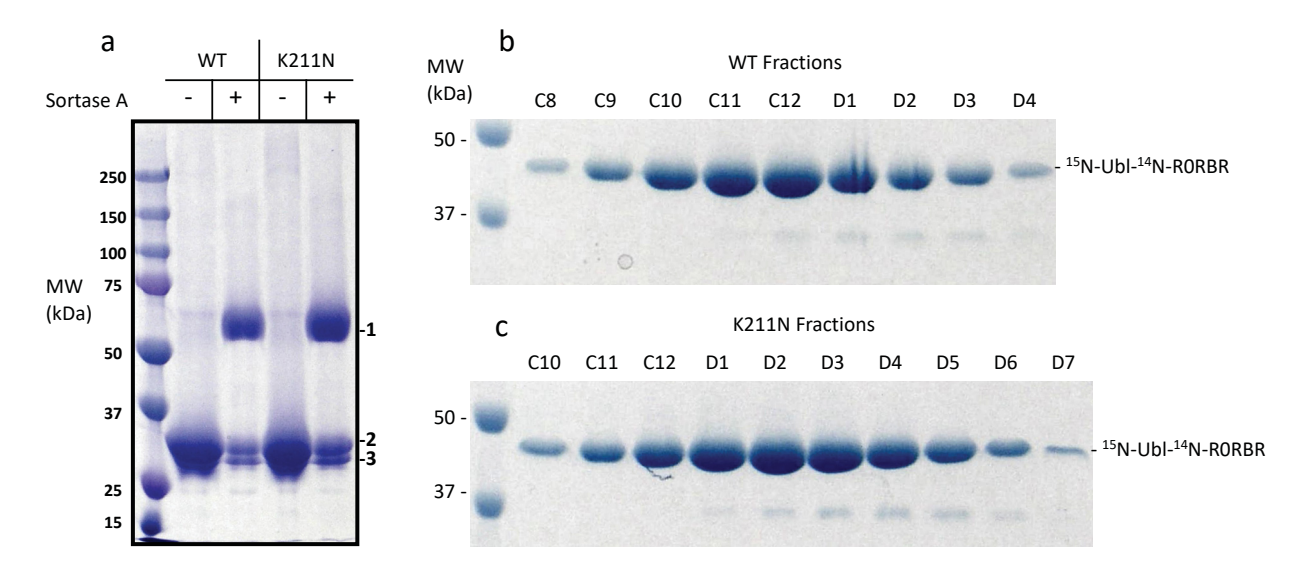


Figure 13: Sortase A ligation of ¹⁵N-Ubl and ¹⁴N-R0RBR.

a, The reaction was dialyzed in buffer overnight at 4 °C. Band 1 corresponds to full length segmentally labeled parkin. Band 2 correspond to ¹⁵N-GST-Ubl. Band 3 corresponds to ¹⁴N-ΔUbl. b, Purification fractions of the sortase A reaction of WT parkin from size exclusion chromatography. c, Purification fractions of the sortase A reaction of K211N mutant from size exclusion chromatography.

The signals from segmentally labeled parkin were strongly attenuated due to the high molecular weight of full-length parkin. Nonetheless, we were able to use the signal intensity as a proxy for the strength of Ubl domain binding to other domains of parkin. In the absence of activation, the Ubl domain was bound to RING1 and yielded a weak NMR spectrum (Figure 12b). Phosphorylated parkin also showed strongly attenuated signals due to pUbl binding to the RING0 domain (Figure 12b). On the other hand, upon phosphorylation, the spectrum of the K211N mutant was very similar to that of free ¹⁵N-pUbl, indicating that the pUbl domain remained largely unbound.

3.4 Resolving conflicting models of Parkin activation

Kumar and colleagues (Kumar et al., 2017) recently proposed that parkin may function as a dimer where the RING2 domain binds to a second parkin molecule bound to a charged E2~Ub

complex (Figure 14a). Alternatively, mobility of the catalytic RING2 domain would allow the RING2 domain to reach the E2~Ub complex bound to the same parkin molecule. To discriminate between these two models (*trans* or *cis*) of catalysis, we performed an autoubiquitination assay using a mixture of two parkin mutants that disrupt E2 binding (A240R) and thioester formation (C431A). Upon phosphorylation, wild-type parkin demonstrated robust activity in the presence of pUb and UbcH7, while the mutants demonstrated little or no activity (Figure 14b). The mixture of both mutants did not rescue activity, suggesting that parkin activation occurs only in *cis*. This is consistent with previous reports showing that pParkin-pUb-UbcH7~Ub assemble as a heterotrimer on size-exclusion chromatography (Ordureau et al., 2015; Kumar et al., 2017).

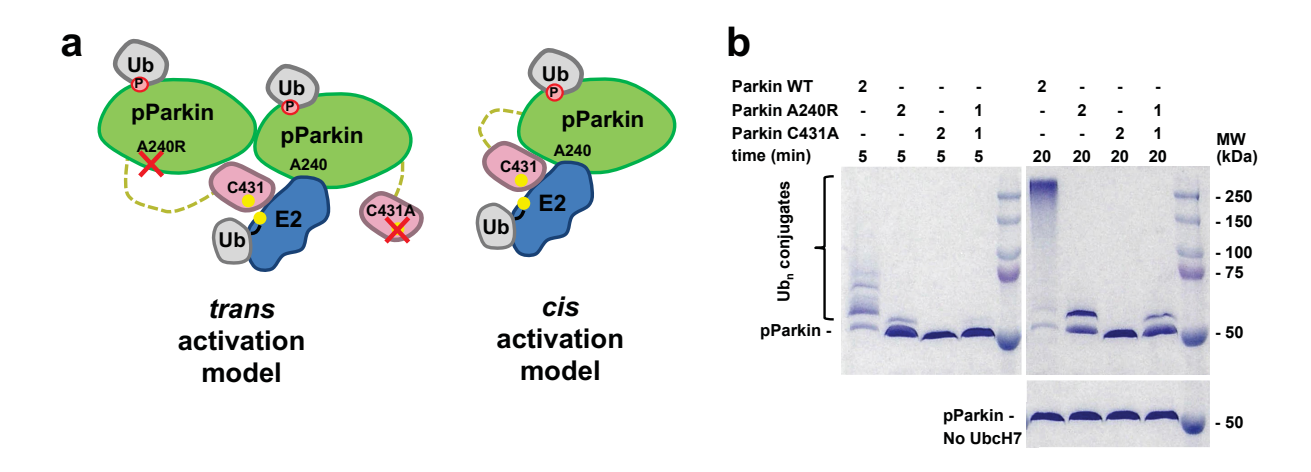


Figure 14: Complementary assay resolving conflicting model. a, Alternative models for thioester transfer in activated parkin. b, Autoubiquitination assay with rat phospho-parkin WT, A240R, or C431A shows the absence of *trans* complementation by E2-binding and catalytic site parkin mutants (concentrations in μ M).

3.5 Parkin phosphorylation is required to free up RING2

We performed HDX mass spectrometry (HDX-MS) experiments (Okiyoneda et al., 2013; Calles-Garcia et al., 2017) to validate that the major conformational changes observed in parkin crystal structure occur in solution (Figure 15). HDX-MS experiments allow mapping of the

deuterium exchange rate with a resolution that depends on the peptide coverage, which was roughly 15 amino acids in our case. The exchange rate depends on solvent exposure and protein stability. We used HDX-MS to address the effects of pUb binding, Ubl phosphorylation, and the loss of pUbl binding site on the structure of rat parkin.

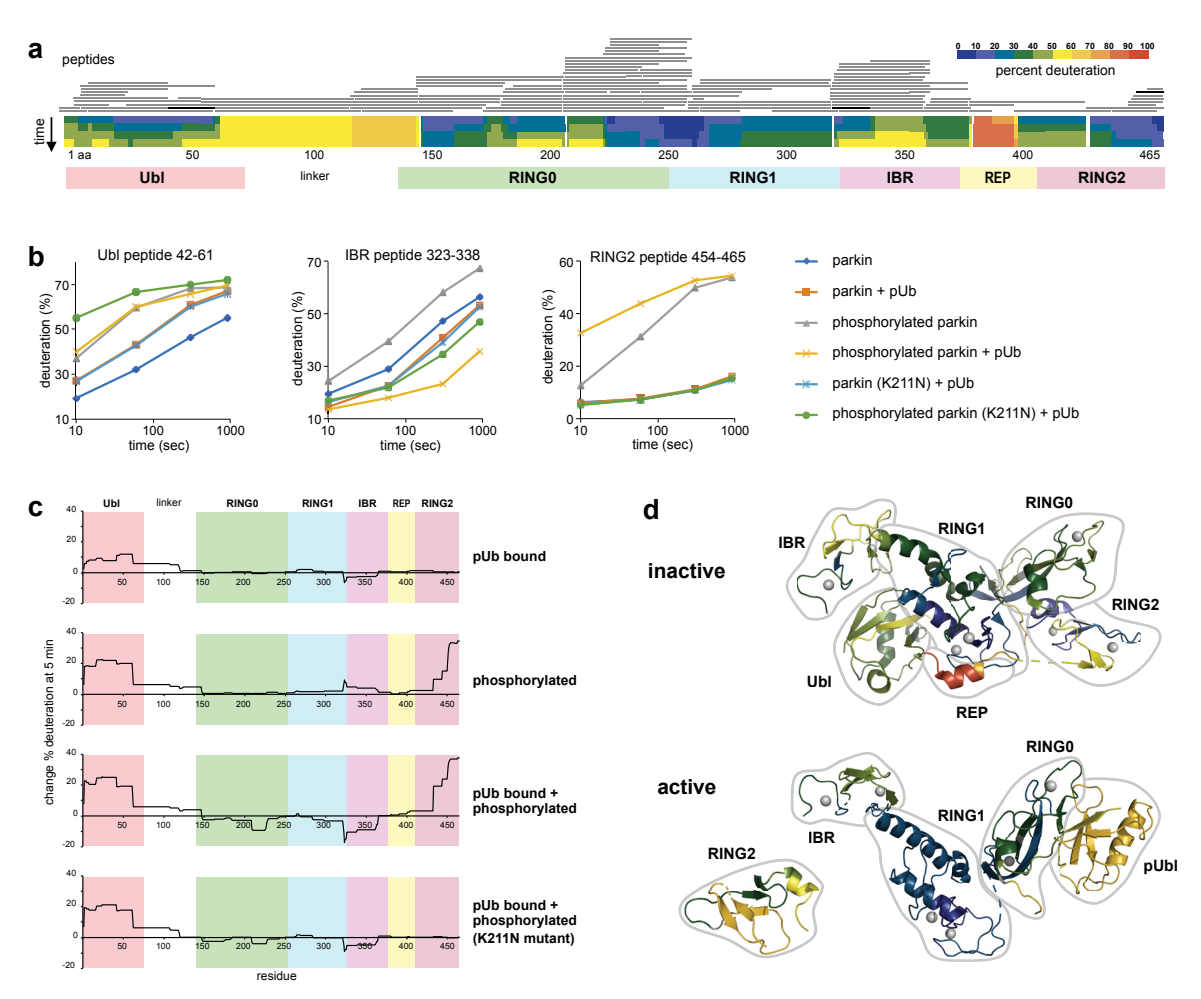


Figure 15. HDX-MS detection of conformational changes upon activation of rat parkin by phosphorylation and phospho-ubiquitin binding.

a, Peptide coverage and deuteration of inactive parkin at four different time points. The Ubl-RING0 and REP linkers show the fastest exchange while the RING0, RING1, and RING2 domains show the slowest. b, Time course of deuteration of three peptides in the six different conformational states. Parkin activation increases exchange in the Ubl and RING2 peptides but slows exchange in the IBR peptide. The RING2 peptide 454-465 shows the largest HDX change. c, Differences in exchange rates following different steps of activation. The K211N mutation in the pUbl-binding site completely blocks the increase in deuteration in response to parkin phosphorylation. d, Mapping of deuteration at 5 min onto the structures of parkin (PDB 4K95 and this work) illustrates the changes in HDX upon activation by pUb binding and phosphorylation. The active RING2 structure is a model.

HDX-MS analysis of parkin in its autoinhibited, inactive conformation showed agreement between the deuteration rates and the crystal structure (Figure 15a,d) (Trempe et al., 2013). The Ubl and other structured domains showed low levels of deuteration while the two linkers showed extensive deuteration. The differences between the linkers are due to back-exchange during the MS analysis. Addition of pUb led to substantial changes in the deuteration pattern (Figure 15b, c). The parkin Ubl showed increased exchange in agreement with the loss of Ubl-RING1 binding observed previously in small-angle X-ray scattering, NMR, and phosphorylation experiments (Kazlauskaite et al., 2015; Sauvé et al., 2015; Kumar et al., 2017). The effect of pUb binding could also be seen on the exchange in the IBR domain. The peptide comprising residues 323-338 showed markedly less exchange upon addition of pUb to either parkin or phosphorylated parkin. In contrast, pUb addition had no effect on deuteration of peptides from RING2.

The phosphorylation of the parkin Ubl domain induced distinct changes in the deuteration pattern (Figure 15b, c). The phosphorylated Ubl domain showed more exchange than was observed upon pUb binding. This likely reflects both the release of the phosphorylated Ubl from its binding site on RING1 (Sauvé et al., 2015) and the structural destabilization of the Ubl domain (Aguirre et al., 2017). Parkin phosphorylation also slightly increased the rate of deuteration of RING1 and IBR domains possibly due to loss of Ubl binding to RING1.

The largest changes were in the RING2 domain (Figure 15c). Parkin phosphorylation greatly increased deuteration of the C-terminal helix both in the presence and absence of pUb. Examination of the structures of parkin explains the large change in RING2 deuteration (Figure 15d). In the inactive structure, the C-terminal helix is tightly bound to RING0 and protected from solvent. Upon release, the helix is fully exposed and undergoes rapid exchange. This is consistent with a model of parkin activation through the phosphorylation-dependent release of RING2. The

combination of pUb binding and parkin phosphorylation modestly enhanced the effects of both individual changes. Although small, the differences are substantially larger than the variation between technical repeats. The Ubl and RING2 domains show faster exchange and the RING1 and IBR domains show slower exchange. The synergy suggests some coupling between pUb binding and parkin activation in agreement with previous studies (Sauvé et al., 2015; Kumar et al., 2015; Ordureau et al., 2014).

The most striking confirmation of our activation model comes from HDX-MS analysis of the K211N parkin mutant, which is impaired in pUbl binding to RING0. Exchange rates for wild-type parkin and the K211N mutant in the presence of pUb were indistinguishable (Figure 15b). However, the effects of parkin phosphorylation were dramatically different. Loss of the pUbl binding site on RING0 completely blocked the increase in RING2 exchange (Figure 15c). At the shorter time point, the Ubl peptide 42-61 in phosphorylated parkin showed faster exchange in the K211N mutant than wild-type due to the inability of the mutated RING0 to bind pUbl (Figure 15b). Analysis of the mutant also illustrates the reproducibility of the HDX-MS analysis; in the absence of phosphorylation, the deuteration rates of wild-type + pUb and K211N parkin + pUb were identical (Figure 15).

3.6 pUb activation of Parkin

When we first performed the NMR experiments to verify pUbl binding site, we added an excess amount of pUb to R0RBR. We then added ¹⁵N-labeled pUbl to the mixture expecting the loss of signal; however, there was no weakening of signals. Since pUb and pUbl are structurally similar, we hypothesized that the pUb was binding to the same region as the pUbl domain on

RING0. Therefore, we lowered the pUb concentration and observed the weakening of pUbl signals (Figure 16). This suggests that pUb could actually bind to RING0 aside from RING1.

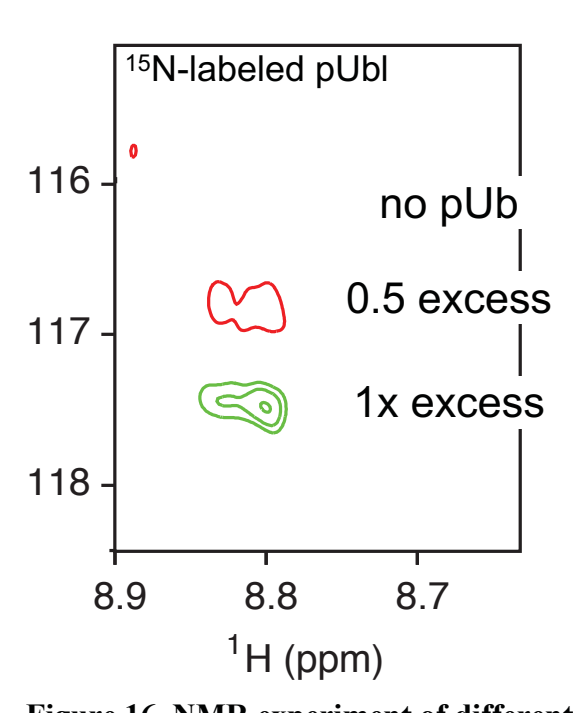


Figure 16. NMR experiment of different amount of pUb Comparison of spectra of the isolated 15 N-labeled pUbl domain in the presence of Δ Ubl-parkin and different amounts of pUb. The spectra were shifted for comparison. pUbl binding to parkin

results in loss of the amide signal from phosphoserine 65 (pSer65).

To further investigate how well pUb could activate parkin, I decided to perform a UbVS assay. The UbVS assay uses a ubiquitin modified at the C terminus with vinyl sulfone that reacts covalently with the active cysteine of parkin. This assay will allow us to observe the degree of RING2 release. First, the R0RBRs, of both wild type and K211N mutant, were co-purified with pUb in order to get the complex binding to RING1. In the assay, different amounts of pUb or pUbl were added to the mixture, and the reaction was performed for 90 minutes (Figure 17 a-c).

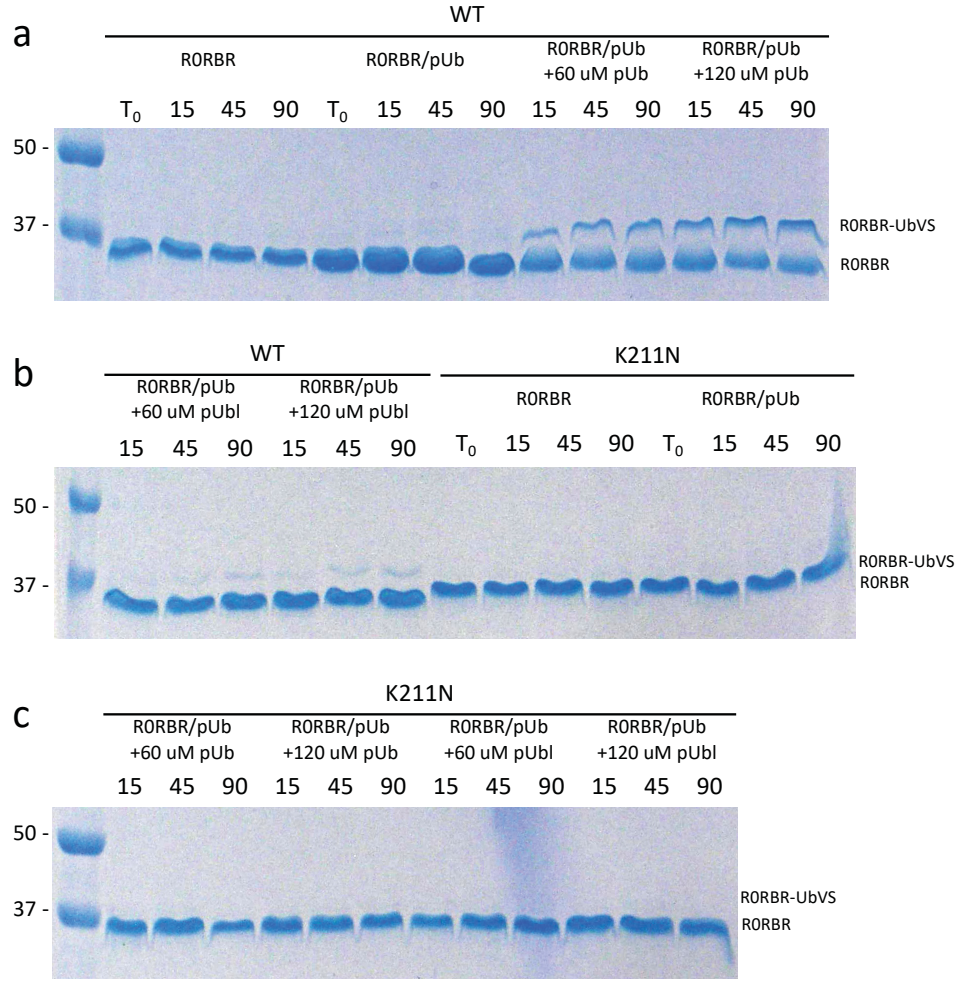


Figure 17: pUb activation of Parkin through RINGO. a-c, UbVS assay showing that pUb and pUbl activate R0RBR. From the gel, pUb activates R0RBR much better than pUbl. When same reaction was done with the K211N mutant, there was no activity observed.

From the assay, pUb and pUbl do indeed bind to the same position because when the RING0 site was mutated, there was no activity with either pUb or pUbl. However, to our surprise, pUb reactions showed higher amount of coupling of the UbVS, suggesting that there was much a higher activity in this case. Since this result is still preliminary, more experiments need to be conducted to understand the intricacies of parkin activation through the RING0 domain.

4. Discussion

To restrict their ubiquitination function, most RBR E3 ligases are autoinhibited when their activity is not required. Although the ligases share the same core domains, their autoinhibition arises from different intra- and/or inter-molecular interactions (Duda et al., 2013; Trempe et al., 2013; Wauer et al., 2013; Riley et al., 2013; Kelsall et al., 2013; Ho et al., 2015; Smit et al., 2012; Stieglitz et al., 2012). RBR E3 ligases bind E2 enzymes through their RING1 domains but this interaction occurs at different stages of their activation. HHARI can bind E2~Ub while inactive, whereas the parkin E2-binding site only becomes accessible once parkin is activated (Sauvé et al., 2015; Trempe et al., 2013; Pao et al., 2016; Lazarou et al., 2013). Inhibition also occurs at the stage of ubiquitin transfer to the catalytic site. In HHARI, inhibition arises from occlusion of the RING2 domain by the adjacent Ariadne domain (Dove et al., 2017). In parkin, the RING0 blocks the catalytic site.

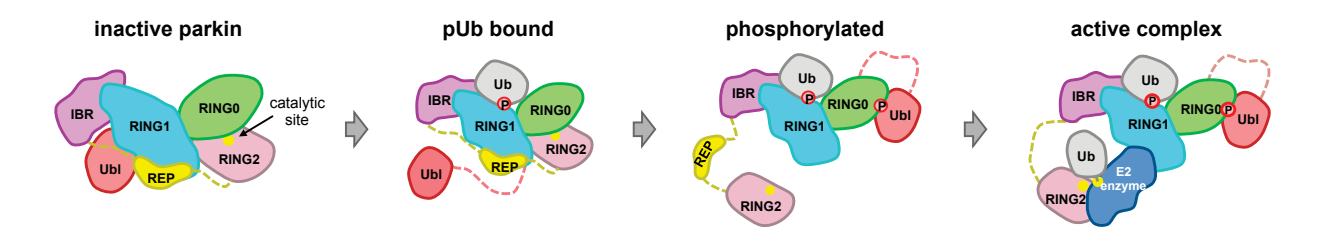


Figure 18. Pathway of parkin activation.

pUb binding primes parkin for phosphorylation by PINK1 by releasing the Ubl domain. Once phosphorylated, the Ubl domain binds to RING0 to release the RING2 domain for catalysis with ubiquitin-charged E2 enzyme.

The inactive and active parkin structures suggest a model for parkin activation (Figure 18). In a first step, inactive parkin binds to phosphorylated ubiquitin generated by PINK1 on the mitochondrial outer membrane (Ordureau et al., 2014; Tang et al., 2017). Phospho-ubiquitin binding decreases the association of the Ubl domain with RING1 and, in the presence of PINK1, the dissociated Ubl domain is efficiently phosphorylated (Sauvé et al., 2015; Kumar et al., 2015;

Rasool et al., 2018; Wauer et al., 2015; Pao et al., 2016; Caulfield et al., 2014). The phosphorylated Ubl domain then binds to RING0 and the steric clash leads to release of the RING2 domain and adjacent REP linker. With both the Ubl and REP elements removed from RING1, parkin is free to bind the E2~Ub enzyme conjugate. The RING2, which remains tethered to the IBR domain, is free to dock with the E2~Ub enzyme to catalyze the transfer of ubiquitin from the E2 to RING2. This obviates the requirement for dimerization to bring the E2 and RING2 catalytic sites together. How the second catalytic step – transfer of ubiquitin to protein substrates – occurs is not known. Substrates could interact with the ubiquitin-charged RING2 while in contact with the E2 or the RING2 domain could dissociate before transferring ubiquitin to substrates.

One may wonder how the pUbl domain can bind prior to the dissociation of the RING2 domain. Many lines of evidence suggest that parkin undergoes dynamic domain movements. Firstly, although the PINK1-binding surface is not available in the inactive conformation, parkin can be phosphorylated in the absence of pUb, albeit less efficiently (Ordureau et al., 2014; Sauvé et al., 2015; Pao et al., 2016). Secondly, inactive parkin shows elevated HDX for the REP helix even at 10 seconds, suggesting a rapid exchange between bound and unbound states (Figure 15a). Thirdly, unmodified parkin shows residual ubiquitination activity (Trempe et al., 2013), suggesting that RING2 spontaneously dissociates even in the absence of phosphorylation. Indeed, the interaction surface between RING0 and RING2 is only 1356 Å² and formed mostly by van der Waals interactions, which suggest a low energy barrier for dissociation. Finally, a molecular dynamics simulation suggested that Ubl phosphorylation could induce the spontaneous dissociation auto-inhibitory elements in parkin (Caulfield et al., 2014). Rather than all-or-nothing transitions, parkin activation is a shift in a dynamic equilibrium mediated by pUb binding and parkin phosphorylation.

Previous mutagenesis results corroborate this model. We observed that mutations that disrupt the RING0-RING2 interface (F146A, F463A) or weaken the REP-RING1 interface (W403A) promote parkin activity both *in vitro* and *in vivo* (Trempe et al., 2013; Tang et al., 2017). These mutants rescue the S65A parkin mutation, implying that they act downstream of parkin phosphorylation. The parkin C457S mutant also shows hyperactivity, which is surprising since the residue is involved in coordinating a Zn²⁺ atom in the catalytic RING2 domain (Trempe et al., 2013). We attribute its hyperactivity to perturbation of the RING2-RING0 interface in agreement with our observation of a large increase in HDX around Cys457 upon parkin phosphorylation (Figure 15c).

Although dominated by large domain movements, allosteric interactions within domains also exist in the pathway. The best understood is the conformational change in the RING1 domain that couples parkin phosphorylation and pUb binding (Figure 6d). Parkin affinity for pUb increases roughly 15-fold when the Ubl domain is deleted or parkin is phosphorylated (Sauvé et al., 2015; Kumar et al., 2015; Ordureau et al., 2014). Conversely, parkin is more easily phosphorylated when pUb is bound (Sauvé et al., 2015; Wauer et al., 2015; Ordureau et al., 2018). This coupling is visible in the HDX data where pUb binding induces an increase in solvent exposure of the Ubl domain (Figure 15c). Previous studies have shown that E2 binding and RING2 dissociation are coupled; the W403A mutation that dissociates the REP linker increases the reactivity of Cys431 for Ub-vinyl sulfone (Tang et al., 2017), similarly to parkin phosphorylation or activating mutations in RING2 (Riley et al., 2013; Ordureau et al., 2014). Likewise, parkin phosphorylation opens the E2-binding site on RING1 and enhances the affinity of E2 binding to parkin (Sauvé et al., 2015). Recently, a section of the linker (named the activating element, or ACT) between the Ubl and RING0 was found to bind RING0 and pUbl in the active conformation of parkin

(Gladkova et al., 2018). It was shown that the ACT element stabilizes the active conformation of parkin through the interaction with the hydrophobic patch on RING0, which is the same patch that binds RING2. The ACT element reportedly stimulates parkin activity but is only conserved in chordates; *Bactrocera* parkin displays robust activity without an ACT. Moreover, human and rat parkin with large deletions in the linker demonstrate robust phosphorylation-dependent E3 ligase activity (Kumar et al., 2015; Sauvé et al., 2015). More studies are required to determine the importance of the ACT linker in fine-tuning parkin regulation.

Some may argue that the domain movements we observe are due to E2 binding. However, several arguments suggest that E2 binding plays a minor role in the conformational changes. Firstly, the crystal structure does not show contacts of the E2 domain outside of RING1. There are no structural changes in RING1 relative to the structure of *Pediculus humanus* parkin with pUb bound (Wauer et al., 2015). Secondly, we see clear evidence of pUbl binding to RING0 and release of the RING2 domain in NMR and HDX experiments in the absence of added E2. Thirdly, in cells, recruitment of E2 enzymes such as UbcH7 takes place only when parkin is first recruited to depolarized mitochondria, suggesting activated parkin recruits E2 rather than the opposite (Geisler et al., 2014).

In addition, indirect evidence suggests the ubiquitin makes additional contacts with parkin even though the ubiquitin moiety of E2~Ub is missing from our structure. Firstly, activated parkin has a higher affinity for E2~Ub than the E2 alone (Kumar et al., 2015); this interaction requires Glu321, which is part of a cryptic ubiquitin-binding site formed by the IBR and RING1 C-terminal helix (Kumar et al., 2017). Secondly, the rate of hydrolysis of the thioester bond in UbcH7~Ub is slowed by the addition of catalytically inactive C431A parkin (Trempe et al., 2013). Parkin contacts affecting the conformation of the E2~Ub linkage (Wenzel et al., 2011; Dove et al., 2017)

or RING2 binding are the most likely explanations. In the HHARI-UbcH7~Ub and HOIP-UbcH5B~Ub structures, RING1 and IBR contacts are present and thought to fix the E2~Ub conformation to favor ubiquitin transfer to the RBR catalytic site (Dove et al., 2017; Lechtenberg et al., 2016; Yuan et al., 2017). It is also possible that differences exist between E2s conjugates. Characterization of multiple RBR ligases found UbcH5~Ub binding requires an interaction with ubiquitin while recognition of UbcH7~Ub is driven primarily by E2-RING1 contacts (Martino et al., 2018).

From our data, pUbl was shown to be important for relieving RING2 from binding to RING0, but it may not be the only way for RING2 to be released. A previous study showed that parkin recruitment was not completely impaired when the Ubl domain was deleted (Ordureau et al., 2014). Moreover, it was also shown that R0RBR can be activated in the presence of pUb (Kazlauskaite et al., 2014). It could be reasoned that pUbl is the main activating domain due to the local concentration; however, after mass recruitment of parkin to the mitochondria, pUb could act as a buffering activator before the Ubl domain was phosphorylated. This provides us with another perspective regulatory system for parkin. Not only can parkin be activated by its own pUbl, but parkin could also be activated in the presence of excess amounts of pUb.

Finally, our results are consistent with the low substrate and chain type specificity of parkin (Ordureau et al., 2014; Cunningham et al., 2015). Once released from RING0, the catalytic domain is highly mobile and constrained only by the ~30 amino acid IBR-RING2 linker. While precise positioning of the activated and acceptor ubiquitin molecules is responsible for the chain specificity of ligases such as HOIP (Lechtenberg et al., 2016), parkin generates a variety of chain types. Similarly, the broad spectrum of substrates that parkin can ubiquitinate (Sarraf et al., 2013) suggests that its substrates are defined by proximity rather than by specific contacts.

While we have understood how parkin is activated through phosphorylation, more interactions need to be studied, such as RING0 regulation, E2~Ub/parkin interaction, and parkin-substrate interaction. For RING0 regulation, binding assays such as NMR experiment will be able to show how pUb or pUbl regulates parkin activity. X-ray crystallization will be able to show us how RING2 interacts with E2~Ub. However, other techniques such as the ITC can also show the binding affinity of E2~Ub with parkin. These two combinations of studies can further the project by providing insight into downstream ubiquitination reaction. Furthermore, from the recent discovery of parkin's role in immune response, there is still a lot that can be learned. The interactions between parkin and proteins involved in MitAP and MDV will be important to understand how parkin is involved in the autoimmune response. Although it has been found that Snx9 is degraded in a parkin-dependent manner, the degradation pathway of Snx9 is still unclear. By studying the interactions between parkin and other interacting partners, we might uncover new target sites for pharmacological therapy.

5. References

- Abbas, N., Lucking, C. B., Ricard, S., Durr, A., Bonifati, V., De Michele, G., Bouley, S., Vaughan, J. R., Gasser, T., Marconi, R., Broussolle, E., Brefel-Courbon, C., Harhangi, B. S., Oostra, B. A., Fabrizio, E., Bohme, G. A., Pradier, L., Wood, N. W., Filla, A., Meco, G., Denefle, P., Agid, Y., & Brice, A. (1999). A wide variety of mutations in the parkin gene are responsible for autosomal recessive parkinsonism in Europe. French Parkinson's Disease Genetics Study Group and the European Consortium on Genetic Susceptibility in Parkinson's Disease. *Human Molecular Genetics*, 8(4), 567-574.
- Adams, P. D., Afonine, P. V., Bunkóczi, G., Chen, V. B., Davis, I. W., Echols, N., Headd, J. J., Hung, L.-W., Kapral, G. J., Grosse-Kunstleve, R. W., McCoy, A. J., Moriarty, N. W., Oeffner, R., Read, R. J., Richardson, D. C., Richardson, J. S., Terwilliger, T. C., & Zwart, P. H. (2010). PHENIX: a comprehensive Python-based system for macromolecular structure solution. *Acta Crystallographica Section D: Biological Crystallography*, 66(Pt 2), 213-221.
- Afonine, P. V., Grosse-Kunstleve, R. W., Echols, N., Headd, J. J., Moriarty, N. W., Mustyakimov, M., Terwilliger, T. C., Urzhumtsev, A., Zwart, P. H., & Adams, P. D. (2012). Towards automated crystallographic structure refinement with phenix.refine. *Acta Crystallographica Section D: Biological Crystallography*, 68(Pt 4), 352-367.
- Aguirre, J. D., Dunkerley, K. M., Mercier, P., & Shaw, G. S. (2017). Structure of phosphorylated UBL domain and insights into PINK1-orchestrated parkin activation. *Proceedings of the National Academy of Sciences of the United States of America*, 114(2), 298-303.
- Anderson, J. P., Walker, D. E., Goldstein, J. M., de Laat, R., Banducci, K., Caccavello, R. J., Barbour, R., Huang, J., Kling, K., Lee, M., Diep, L., Keim, P. S., Shen, X., Chataway, T., Schlossmacher, M. G., Seubert, P., Schenk, D., Sinha, S., Gai, W. P., & Chilcote, T. J. (2006). Phosphorylation of Ser-129 is the dominant pathological modification of alphasynuclein in familial and sporadic Lewy body disease. *Journal of Biological Chemistry*, 281(40), 29739-29752.
- Baden, P., Yu, C., & Deleidi, M. (2019). Insights into GBA Parkinson's disease pathology and therapy with induced pluripotent stem cell model systems. *Neurobiology of Disease*, 127, 1-12.
- Bai, Y., Milne, J. S., Mayne, L., & Englander, S. W. (1993). Primary structure effects on peptide group hydrogen exchange. *Proteins*, 17(1), 75-86.
- Barbeau, A. (1969). L-dopa therapy in Parkinson's disease: a critical review of nine years' experience. *Canadian Medical Association journal*, 101(13), 59-68.

- Berndsen, C. E., & Wolberger, C. (2014). New insights into ubiquitin E3 ligase mechanism. *Nature Structural & Molecular Biology*, 21(4), 301-307.
- Birkmayer, W., & Hornykiewicz, O. (1961). [The L-3,4-dioxyphenylalanine (DOPA)-effect in Parkinson-akinesia]. *Wien Klin Wochenschr*, 73, 787-788.
- Calles-Garcia, D., Yang, M., Soya, N., Melero, R., Menade, M., Ito, Y., Vargas, J., Lukacs, G. L., Kollman, J. M., Kozlov, G., & Gehring, K. (2017). Single-particle electron microscopy structure of UDP-glucose:glycoprotein glucosyltransferase suggests a selectivity mechanism for misfolded proteins. *Journal of Biological Chemistry*, 292(27), 11499-11507.
- Caulfield, T. R., Fiesel, F. C., Moussaud-Lamodière, E. L., Dourado, D. F. A. R., Flores, S. C., & Springer, W. (2014). Phosphorylation by PINK1 Releases the UBL Domain and Initializes the Conformational Opening of the E3 Ubiquitin Ligase Parkin. *PLoS Computational Biology*, 10(11), e1003935.
- Charcot, J. (1892). La médicine vibratoire: Application des vibrations rapides et continues a traitement de quelques maladies du système nerveux. *Prog Méd, 16*, 149-151.
- Chau, V., Tobias, J. W., Bachmair, A., Marriott, D., Ecker, D. J., Gonda, D. K., & Varshavsky, A. (1989). A multiubiquitin chain is confined to specific lysine in a targeted short-lived protein. *Science*, 243(4898), 1576.
- Chaugule, V. K., Burchell, L., Barber, K. R., Sidhu, A., Leslie, S. J., Shaw, G. S., & Walden, H. (2011). Autoregulation of Parkin activity through its ubiquitin-like domain. *The EMBO Journal*, 30(14), 2853-2867.
- Chen, Z. J., Niles, E. G., & Pickart, C. M. (1991). Isolation of a cDNA encoding a mammalian multiubiquitinating enzyme (E225K) and overexpression of the functional enzyme in Escherichia coli. *Journal of Biological Chemistry*, 266(24), 15698-15704.
- Cotzias, G. C., Papavasiliou, P. S., & Gellene, R. (1969). Modification of Parkinsonism Chronic Treatment with L-Dopa. *New England Journal of Medicine*, 280(7), 337-345.
- Cunningham, C. N., Baughman, J. M., Phu, L., Tea, J. S., Yu, C., Coons, M., Kirkpatrick, D. S., Bingol, B., & Corn, J. E. (2015). USP30 and parkin homeostatically regulate atypical ubiquitin chains on mitochondria. *Nature Cell Biology*, *17*(2), 160-169.
- Delaglio, F., Grzesiek, S., Vuister, G. W., Zhu, G., Pfeifer, J., & Bax, A. (1995). NMRPipe: A multidimensional spectral processing system based on UNIX pipes. *Journal of Biomolecular NMR*, 6(3), 277-293.

- Deng, H., Wang, P., & Jankovic, J. (2018). The genetics of Parkinson disease. *Ageing Research Review*, 42, 72-85.
- DeWitt, D. C., & Rhoades, E. (2013). alpha-Synuclein can inhibit SNARE-mediated vesicle fusion through direct interactions with lipid bilayers. *Biochemistry*, *52*(14), 2385-2387.
- Dove, K. K., & Klevit, R. E. (2017). RING-Between-RING E3 Ligases: Emerging Themes amid the Variations. *Journal of Molecular Biology*, 429(22), 3363-3375.
- Dove, K. K., Olszewski, J. L., Martino, L., Duda, D. M., Wu, X. S., Miller, D. J., Reiter, K. H., Rittinger, K., Schulman, B. A., & Klevit, R. E. (2017). Structural Studies of HHARI/UbcH7 approximately Ub Reveal Unique E2 approximately Ub Conformational Restriction by RBR RING1. *Structure*, *25*(6), 890-900 e895.
- Dove, K. K., Stieglitz, B., Duncan, E. D., Rittinger, K., & Klevit, R. E. (2016). Molecular insights into RBR E3 ligase ubiquitin transfer mechanisms. *EMBO Reports*, 17(8), 1221.
- Duda, D. M., Olszewski, J. L., Schuermann, J. P., Kurinov, I., Miller, D. J., Nourse, A., Alpi, A. F., & Schulman, B. A. (2013). Structure of HHARI, a RING-IBR-RING ubiquitin ligase: autoinhibition of an Ariadne-family E3 and insights into ligation mechanism. *Structure* (London, England: 1993), 21(6), 1030-1041.
- Emsley, P., Lohkamp, B., Scott, W. G., & Cowtan, K. (2010). Features and development of Coot. *Acta Crystallogr D Biol Crystallogr*, 66(Pt 4), 486-501.
- Engelhardt, E., & Gomes, M. d. M. (2017). Lewy and his inclusion bodies: Discovery and rejection. *Dementia & neuropsychologia*, 11(2), 198-201.
- Funayama, M., Hasegawa, K., Kowa, H., Saito, M., Tsuji, S., & Obata, F. (2002). A new locus for Parkinson's disease (PARK8) maps to chromosome 12p11.2–q13.1. *Annals of Neurology*, 51(3), 296-301.
- Geisler, S., Holmstrom, K. M., Skujat, D., Fiesel, F. C., Rothfuss, O. C., Kahle, P. J., & Springer, W. (2010). PINK1/Parkin-mediated mitophagy is dependent on VDAC1 and p62/SQSTM1. *Nature Cell Biology*, *12*(2), 119-131.
- Geisler, S., Vollmer, S., Golombek, S., & Kahle, P. J. (2014). UBE2N, UBE2L3 and UBE2D2/3 ubiquitin-conjugating enzymes are essential for parkin-dependent mitophagy. *Journal of Cell Science*.
- Gladkova, C., Maslen, S., Skehel, J. M., & Komander, D. (2018). Mechanism of parkin activation by PINK1. *Nature*.

- Goetz, C. G. (2011). The history of Parkinson's disease: early clinical descriptions and neurological therapies. *Cold Spring Harbor perspectives in medicine*, *I*(1), a008862-a008862.
- Greggio, E., Zambrano, I., Kaganovich, A., Beilina, A., Taymans, J. M., Daniels, V., Lewis, P., Jain, S., Ding, J., Syed, A., Thomas, K. J., Baekelandt, V., & Cookson, M. R. (2008). The Parkinson disease-associated leucine-rich repeat kinase 2 (LRRK2) is a dimer that undergoes intramolecular autophosphorylation. *Journal of Biological Chemistry*, 283(24), 16906-16914.
- Hattori, N., Matsumine, H., Asakawa, S., Kitada, T., Yoshino, H., Elibol, B., Brookes, A. J., Yamamura, Y., Kobayashi, T., Wang, M., Yoritaka, A., Minoshima, S., Shimizu, N., & Mizuno, Y. (1998). Point mutations (Thr240Arg and Gln311Stop) [correction of Thr240Arg and Ala311Stop] in the Parkin gene. *Biochemical and Biophysical Research Communications*, 249(3), 754-758.
- Ho, S. R., Lee, Y. J., & Lin, W. C. (2015). Regulation of RNF144A E3 Ubiquitin Ligase Activity by Self-association through Its Transmembrane Domain. *Journal of Biological Chemistry*, 290(38), 23026-23038.
- James Parkinson, Member of the Royal College of Surgeons. (2002). An Essay on the Shaking Palsy. *The Journal of Neuropsychiatry and Clinical Neurosciences*, *14*(2), 223-236.
- Kabsch, W. (2010). Xds. *Acta Crystallographica Section D: Biological Crystallography*, 66(Pt 2), 125-132.
- Kane, L. A., Lazarou, M., Fogel, A. I., Li, Y., Yamano, K., Sarraf, S. A., Banerjee, S., & Youle, R. J. (2014). PINK1 phosphorylates ubiquitin to activate Parkin E3 ubiquitin ligase activity. *Journal of Cell Biology*, 205(2), 143-153.
- Kazlauskaite, A., Kondapalli, C., Gourlay, R., Campbell, David G., Ritorto, Maria S., Hofmann, K., Alessi, Dario R., Knebel, A., Trost, M., & Muqit, Miratul M. K. (2014). Parkin is activated by PINK1-dependent phosphorylation of ubiquitin at Ser65. *Biochemical Journal*, 460(1), 127-141.
- Kazlauskaite, A., Martínez-Torres, R. J., Wilkie, S., Kumar, A., Peltier, J., Gonzalez, A., Johnson, C., Zhang, J., Hope, A. G., Peggie, M., Trost, M., van Aalten, D. M. F., Alessi, D. R., Prescott, A. R., Knebel, A., Walden, H., & Muqit, M. M. K. (2015). Binding to serine 65-phosphorylated ubiquitin primes Parkin for optimal PINK1-dependent phosphorylation and activation. *EMBO Reports*, 16(8), 939-954.
- Kelsall, I. R., Duda, D. M., Olszewski, J. L., Hofmann, K., Knebel, A., Langevin, F., Wood, N., Wightman, M., Schulman, B. A., & Alpi, A. F. (2013). TRIAD1 and HHARI bind to and

- are activated by distinct neddylated Cullin-RING ligase complexes. *The EMBO Journal*, 32(21), 2848-2860.
- Kirisako, T., Kamei, K., Murata, S., Kato, M., Fukumoto, H., Kanie, M., Sano, S., Tokunaga, F., Tanaka, K., & Iwai, K. (2006). A ubiquitin ligase complex assembles linear polyubiquitin chains. *The EMBO Journal*, 25(20), 4877-4887.
- Kitada, T., Asakawa, S., Hattori, N., Matsumine, H., Yamamura, Y., Minoshima, S., Yokochi, M., Mizuno, Y., & Shimizu, N. (1998). Mutations in the parkin gene cause autosomal recessive juvenile parkinsonism. *Nature*, *392*(6676), 605-608.
- Komander, D., & Rape, M. (2012). The ubiquitin code. *Annual Review of Biochemistry*, 81, 203-229.
- Koyano, F., Okatsu, K., Kosako, H., Tamura, Y., Go, E., Kimura, M., Kimura, Y., Tsuchiya, H., Yoshihara, H., Hirokawa, T., Endo, T., Fon, E. A., Trempe, J. F., Saeki, Y., Tanaka, K., & Matsuda, N. (2014). Ubiquitin is phosphorylated by PINK1 to activate parkin. *Nature*, 510(7503), 162-166.
- Kucera, A., Borg Distefano, M., Berg-Larsen, A., Skjeldal, F., Repnik, U., Bakke, O., & Progida, C. (2016). Spatiotemporal Resolution of Rab9 and CI-MPR Dynamics in the Endocytic Pathway. *Traffic*, 17(3), 211-229.
- Kumar, A., Aguirre, J. D., Condos, T. E., Martinez-Torres, R. J., Chaugule, V. K., Toth, R., Sundaramoorthy, R., Mercier, P., Knebel, A., Spratt, D. E., Barber, K. R., Shaw, G. S., & Walden, H. (2015). Disruption of the autoinhibited state primes the E3 ligase parkin for activation and catalysis. *The EMBO Journal*, *34*(20), 2506-2521.
- Kumar, A., Chaugule, V. K., Condos, T. E. C., Barber, K. R., Johnson, C., Toth, R., Sundaramoorthy, R., Knebel, A., Shaw, G. S., & Walden, H. (2017). Parkin-phosphoubiquitin complex reveals a cryptic ubiquitin binding site required for RBR ligase activity. *Nature Structural & Molecular Biology*, 24(5), 475-483.
- Lazarou, M., Narendra, D. P., Jin, S. M., Tekle, E., Banerjee, S., & Youle, R. J. (2013). PINK1 drives Parkin self-association and HECT-like E3 activity upstream of mitochondrial binding. *J Cell Biol*, 200(2), 163-172.
- Lechtenberg, B. C., Rajput, A., Sanishvili, R., Dobaczewska, M. K., Ware, C. F., Mace, P. D., & Riedl, S. J. (2016). Structure of a HOIP/E2~ubiquitin complex reveals RBR E3 ligase mechanism and regulation. *Nature*, *529*(7587), 546-550.
- Lewy, F. H. (1912). Paralysis agitans. I. Pathologische anatomie. Handbuch der neurologie.

- Lin, X., Parisiadou, L., Gu, X. L., Wang, L., Shim, H., Sun, L., Xie, C., Long, C. X., Yang, W. J., Ding, J., Chen, Z. Z., Gallant, P. E., Tao-Cheng, J. H., Rudow, G., Troncoso, J. C., Liu, Z., Li, Z., & Cai, H. (2009). Leucine-rich repeat kinase 2 regulates the progression of neuropathology induced by Parkinson's-disease-related mutant alpha-synuclein. *Neuron*, 64(6), 807-827.
- Liu, Y., Qiang, M., Wei, Y., & He, R. (2011). A novel molecular mechanism for nitrated α-synuclein-induced cell death. *Journal of Molecular Cell Biology*, *3*(4), 239-249.
- Marte, A., Russo, I., Rebosio, C., Valente, P., Belluzzi, E., Pischedda, F., Montani, C., Lavarello, C., Petretto, A., Fedele, E., Baldelli, P., Benfenati, F., Piccoli, G., Greggio, E., & Onofri, F. (2019). Leucine-rich repeat kinase 2 phosphorylation on synapsin I regulates glutamate release at pre-synaptic sites. *Journal of Neurochemistry*, *150*(3), 264-281.
- Martino, L., Brown, N. R., Masino, L., Esposito, D., & Rittinger, K. (2018). Determinants of E2-ubiquitin conjugate recognition by RBR E3 ligases. *Scientific Reports*, 8(1), 68.
- Matheoud, D., Cannon, T., Voisin, A., Penttinen, A. M., Ramet, L., Fahmy, A. M., Ducrot, C., Laplante, A., Bourque, M. J., Zhu, L., Cayrol, R., Le Campion, A., McBride, H. M., Gruenheid, S., Trudeau, L. E., & Desjardins, M. (2019). Intestinal infection triggers Parkinson's disease-like symptoms in Pink1(-/-) mice. *Nature*, *571*(7766), 565-569.
- Matheoud, D., Sugiura, A., Bellemare-Pelletier, A., Laplante, A., Rondeau, C., Chemali, M., Fazel, A., Bergeron, J. J., Trudeau, L.-E., Burelle, Y., Gagnon, E., McBride, H. M., & Desjardins, M. (2016). Parkinson's Disease-Related Proteins PINK1 and Parkin Repress Mitochondrial Antigen Presentation. *Cell*, *166*(2), 314-327.
- Matsuda, N., Sato, S., Shiba, K., Okatsu, K., Saisho, K., Gautier, C. A., Sou, Y. S., Saiki, S., Kawajiri, S., Sato, F., Kimura, M., Komatsu, M., Hattori, N., & Tanaka, K. (2010). PINK1 stabilized by mitochondrial depolarization recruits Parkin to damaged mitochondria and activates latent Parkin for mitophagy. *Journal of Cell Biology*, 189(2), 211-221.
- McCoy, A. J., Grosse-Kunstleve, R. W., Adams, P. D., Winn, M. D., Storoni, L. C., & Read, R. J. (2007). Phaser crystallographic software. *Journal of Applied Crystallography*, 40(Pt 4), 658-674.
- McGinty, R. K., Henrici, R. C., & Tan, S. (2014). Crystal structure of the PRC1 ubiquitylation module bound to the nucleosome. *Nature*, 514(7524), 591-596.
- McLelland, G. L., Soubannier, V., Chen, C. X., McBride, H. M., & Fon, E. A. (2014). Parkin and PINK1 function in a vesicular trafficking pathway regulating mitochondrial quality control. *The EMBO Journal*, 33(4), 282-295.

- Miklossy, J., Arai, T., Guo, J.-P., Klegeris, A., Yu, S., McGeer, E. G., & McGeer, P. L. (2006). LRRK2 Expression in Normal and Pathologic Human Brain and in Human Cell Lines. *Journal of Neuropathology & Experimental Neurology*, 65(10), 953-963.
- Narendra, D. P., Jin, S. M., Tanaka, A., Suen, D. F., Gautier, C. A., Shen, J., Cookson, M. R., & Youle, R. J. (2010). PINK1 is selectively stabilized on impaired mitochondria to activate Parkin. *PLoS Biol*, 8(1), e1000298.
- Okiyoneda, T., Veit, G., Dekkers, J. F., Bagdany, M., Soya, N., Xu, H., Roldan, A., Verkman, A. S., Kurth, M., Simon, A., Hegedus, T., Beekman, J. M., & Lukacs, G. L. (2013). Mechanism-based corrector combination restores DeltaF508-CFTR folding and function. *Nature Chemical Biology*, *9*(7), 444-454.
- Onuaguluchi, G. (1968). Drug treatment of parkinsonism and its assessment. *Handbook of clinical neurology (ed. Vinken PJ, Bruyn GW)*, 6, 218-226.
- Ordureau, A., Heo, J. M., Duda, D. M., Paulo, J. A., Olszewski, J. L., Yanishevski, D., Rinehart, J., Schulman, B. A., & Harper, J. W. (2015). Defining roles of PARKIN and ubiquitin phosphorylation by PINK1 in mitochondrial quality control using a ubiquitin replacement strategy. *Proc Natl Acad Sci U S A*, 112(21), 6637-6642.
- Ordureau, A., Paulo, J. A., Zhang, W., Ahfeldt, T., Zhang, J., Cohn, E. F., Hou, Z., Heo, J. M., Rubin, L. L., Sidhu, S. S., Gygi, S. P., & Harper, J. W. (2018). Dynamics of PARKIN-Dependent Mitochondrial Ubiquitylation in Induced Neurons and Model Systems Revealed by Digital Snapshot Proteomics. *Molecular cell*, 70(2), 211-227 e218.
- Ordureau, A., Sarraf, S. A., Duda, D. M., Heo, J.-M., Jedrychowski, M. P., Sviderskiy, V. O., Olszewski, J. L., Koerber, J. T., Xie, T., Beausoleil, S. A., Wells, J. A., Gygi, S. P., Schulman, B. A., & Harper, J. W. (2014). Quantitative proteomics reveal a feedforward mechanism for mitochondrial PARKIN translocation and ubiquitin chain synthesis. *Molecular cell*, *56*(3), 360-375.
- Pankratz, N., Kissell, D. K., Pauciulo, M. W., Halter, C. A., Rudolph, A., Pfeiffer, R. F., Marder, K. S., Foroud, T., Nichols, W. C., & Parkinson Study Group, P. I. (2009). Parkin dosage mutations have greater pathogenicity in familial PD than simple sequence mutations. Neurology, 73(4), 279-286.
- Pao, K. C., Stanley, M., Han, C., Lai, Y. C., Murphy, P., Balk, K., Wood, N. T., Corti, O., Corvol, J. C., Muqit, M. M., & Virdee, S. (2016). Probes of ubiquitin E3 ligases enable systematic dissection of parkin activation. *Nature Chemical Biology*, 12(5), 324-331.
- Periquet, M., Latouche, M., Lohmann, E., Rawal, N., De Michele, G., Ricard, S., Teive, H., Fraix, V., Vidailhet, M., Nicholl, D., Barone, P., Wood, N. W., Raskin, S., Deleuze, J. F.,

- Agid, Y., Durr, A., & Brice, A. (2003). Parkin mutations are frequent in patients with isolated early-onset parkinsonism. *Brain*, 126(Pt 6), 1271-1278.
- Pickles, S., Vigie, P., & Youle, R. J. (2018). Mitophagy and Quality Control Mechanisms in Mitochondrial Maintenance. *Current Biology*, 28(4), R170-r185.
- Purlyte, E., Dhekne, H. S., Sarhan, A. R., Gomez, R., Lis, P., Wightman, M., Martinez, T. N., Tonelli, F., Pfeffer, S. R., & Alessi, D. R. (2018). Rab29 activation of the Parkinson's disease-associated LRRK2 kinase. *The EMBO Journal*, *37*(1), 1-18.
- Rasool, S., Soya, N., Truong, L., Croteau, N., Lukacs, G. L., & Trempe, J. F. (2018). PINK1 autophosphorylation is required for ubiquitin recognition. *EMBO Reports*, 19(4), e44981.
- Rideout, H. J., & Stefanis, L. (2014). The neurobiology of LRRK2 and its role in the pathogenesis of Parkinson's disease. *Neurochemical Research*, 39(3), 576-592.
- Riley, B. E., Lougheed, J. C., Callaway, K., Velasquez, M., Brecht, E., Nguyen, L., Shaler, T., Walker, D., Yang, Y., Regnstrom, K., Diep, L., Zhang, Z., Chiou, S., Bova, M., Artis, D. R., Yao, N., Baker, J., Yednock, T., & Johnston, J. A. (2013). Structure and function of Parkin E3 ubiquitin ligase reveals aspects of RING and HECT ligases. *Nature Communications*, 4, 1982.
- Safadi, S. S., & Shaw, G. S. (2007). A disease state mutation unfolds the parkin ubiquitin-like domain. *Biochemistry*, 46(49), 14162-14169.
- Sarraf, S. A., Raman, M., Guarani-Pereira, V., Sowa, M. E., Huttlin, E. L., Gygi, S. P., & Harper, J. W. (2013). Landscape of the PARKIN-dependent ubiquitylome in response to mitochondrial depolarization. *Nature*, 496(7445), 372-376.
- Sato, Y., Fujita, H., Yoshikawa, A., Yamashita, M., Yamagata, A., Kaiser, S. E., Iwai, K., & Fukai, S. (2011). Specific recognition of linear ubiquitin chains by the Npl4 zinc finger (NZF) domain of the HOIL-1L subunit of the linear ubiquitin chain assembly complex. *Proceedings of the National Academy of Sciences of the United States of America*, 108(51), 20520-20525.
- Sauvé, V., Lilov, A., Seirafi, M., Vranas, M., Rasool, S., Kozlov, G., Sprules, T., Wang, J., Trempe, J.-F., & Gehring, K. (2015). A Ubl/ubiquitin switch in the activation of Parkin. *The EMBO Journal*, 34(20), 2492-2505.
- Seirafi, M., Kozlov, G., & Gehring, K. (2015). Parkin structure and function. *The FEBS Journal*, 282(11), 2076-2088.

- Shimura, H., Hattori, N., Kubo, S., Mizuno, Y., Asakawa, S., Minoshima, S., Shimizu, N., Iwai, K., Chiba, T., Tanaka, K., & Suzuki, T. (2000). Familial Parkinson disease gene product, parkin, is a ubiquitin-protein ligase. *Nature Genetics*, 25(3), 302-305.
- Shin, N., Lee, S., Ahn, N., Kim, S. A., Ahn, S. G., YongPark, Z., & Chang, S. (2007). Sorting nexin 9 interacts with dynamin 1 and N-WASP and coordinates synaptic vesicle endocytosis. *Journal of Biological Chemistry*, 282(39), 28939-28950.
- Shults, C. W. (2006). Lewy bodies. *Proceedings of the National Academy of Sciences of the United States of America*, 103(6), 1661-1668.
- Sidransky, E., & Lopez, G. (2012). The link between the GBA gene and parkinsonism. *The Lancet Neurology*, 11(11), 986-998.
- Sliter, D. A., Martinez, J., Hao, L., Chen, X., Sun, N., Fischer, T. D., Burman, J. L., Li, Y., Zhang, Z., Narendra, D. P., Cai, H., Borsche, M., Klein, C., & Youle, R. J. (2018). Parkin and PINK1 mitigate STING-induced inflammation. *Nature*, *561*(7722), 258-262.
- Smit, J. J., Monteferrario, D., Noordermeer, S. M., van Dijk, W. J., van der Reijden, B. A., & Sixma, T. K. (2012). The E3 ligase HOIP specifies linear ubiquitin chain assembly through its RING-IBR-RING domain and the unique LDD extension. *The EMBO Journal*, 31(19), 3833-3844.
- Smit, J. J., & Sixma, T. K. (2014). "Ubiquitylation: mechanism and functions" Review series: RBR E3-ligases at work. *EMBO Reports*, 15(2), 142-154.
- Spratt, D. E., Martinez-Torres, R. J., Noh, Y. J., Mercier, P., Manczyk, N., Barber, K. R., Aguirre, J. D., Burchell, L., Purkiss, A., Walden, H., & Shaw, G. S. (2013). A molecular explanation for the recessive nature of parkin-linked Parkinson's disease. *Nature Communications*, *4*, 1983.
- Spratt, Donald E., Walden, H., & Shaw, Gary S. (2014). RBR E3 ubiquitin ligases: new structures, new insights, new questions. *Biochemical Journal*, 458(Pt 3), 421-437.
- Stafa, K., Tsika, E., Moser, R., Musso, A., Glauser, L., Jones, A., Biskup, S., Xiong, Y., Bandopadhyay, R., Dawson, V. L., Dawson, T. M., & Moore, D. J. (2013). Functional interaction of Parkinson's disease-associated LRRK2 with members of the dynamin GTPase superfamily. *Human Molecular Genetics*, 23(8), 2055-2077.
- Steffen, J. D., McCauley, M. M., & Pascal, J. M. (2016). Fluorescent sensors of PARP-1 structural dynamics and allosteric regulation in response to DNA damage. *Nucleic Acids Research*, 44(20), 9771-9783.

- Stieglitz, B., Morris-Davies, A. C., Koliopoulos, M. G., Christodoulou, E., & Rittinger, K. (2012). LUBAC synthesizes linear ubiquitin chains via a thioester intermediate. *EMBO Reports*, 13(9), 840-846.
- Sugiura, A., McLelland, G. L., Fon, E. A., & McBride, H. M. (2014). A new pathway for mitochondrial quality control: mitochondrial-derived vesicles. *The EMBO Journal*, *33*(19), 2142-2156.
- Swatek, K. N., & Komander, D. (2016). Ubiquitin modifications. Cell Research, 26(4), 399-422.
- Tang, M. Y., Vranas, M., Krahn, A. I., Pundlik, S., Trempe, J. F., & Fon, E. A. (2017). Structure-guided mutagenesis reveals a hierarchical mechanism of Parkin activation. *Nature Communications*, 8, 14697.
- Terwilliger, T. C., Adams, P. D., Read, R. J., McCoy, A. J., Moriarty, N. W., Grosse-Kunstleve, R. W., Afonine, P. V., Zwart, P. H., & Hung, L. W. (2009). Decision-making in structure solution using Bayesian estimates of map quality: the PHENIX AutoSol wizard. *Acta Crystallographica Section D: Biological Crystallography*, 65(Pt 6), 582-601.
- Theile, C. S., Witte, M. D., Blom, A. E. M., Kundrat, L., Ploegh, H. L., & Guimaraes, C. P. (2013). Site-specific N-terminal labeling of proteins using sortase-mediated reactions. *Nature Protocols*, *8*, 1800.
- Trempe, J. F., Sauve, V., Grenier, K., Seirafi, M., Tang, M. Y., Menade, M., Al-Abdul-Wahid, S., Krett, J., Wong, K., Kozlov, G., Nagar, B., Fon, E. A., & Gehring, K. (2013). Structure of parkin reveals mechanisms for ubiquitin ligase activation. *Science*, *340*(6139), 1451-1455.
- Trétiakoff, C. (1919). Contribution a l'etude de l'Anatomie pathologique du Locus Niger de Soemmering avec quelques deduction relatives a la pathogenie des troubles du tonus musculaire et de la maladie de Parkinson. *Theses de Paris*.
- Valente, E. M., Abou-Sleiman, P. M., Caputo, V., Muqit, M. M., Harvey, K., Gispert, S., Ali, Z., Del Turco, D., Bentivoglio, A. R., Healy, D. G., Albanese, A., Nussbaum, R., Gonzalez-Maldonado, R., Deller, T., Salvi, S., Cortelli, P., Gilks, W. P., Latchman, D. S., Harvey, R. J., Dallapiccola, B., Auburger, G., & Wood, N. W. (2004). Hereditary early-onset Parkinson's disease caused by mutations in PINK1. Science, 304(5674), 1158-1160.
- Vives-Bauza, C., Zhou, C., Huang, Y., Cui, M., de Vries, R. L., Kim, J., May, J., Tocilescu, M. A., Liu, W., Ko, H. S., Magrane, J., Moore, D. J., Dawson, V. L., Grailhe, R., Dawson, T. M., Li, C., Tieu, K., & Przedborski, S. (2010). PINK1-dependent recruitment of Parkin to mitochondria in mitophagy. *Proceedings of the National Academy of Sciences of the United States of America*, 107(1), 378-383.

- Wang, X., Yan, M. H., Fujioka, H., Liu, J., Wilson-Delfosse, A., Chen, S. G., Perry, G., Casadesus, G., & Zhu, X. (2012). LRRK2 regulates mitochondrial dynamics and function through direct interaction with DLP1. *Human Molecular Genetics*, 21(9), 1931-1944.
- Wauer, T., & Komander, D. (2013). Structure of the human Parkin ligase domain in an autoinhibited state. *The EMBO Journal*, 32(15), 2099-2112.
- Wauer, T., Simicek, M., Schubert, A., & Komander, D. (2015). Mechanism of phosphoubiquitin-induced PARKIN activation. *Nature*, 524(7565), 370-374.
- Wenzel, D. M., Lissounov, A., Brzovic, P. S., & Klevit, R. E. (2011). UbcH7 reactivity profile reveals Parkin and HHARI to be RING/HECT hybrids. *Nature*, 474(7349), 105-108.
- Yahr, M. D., Duvoisin, R. C., Schear, M. J., Barrett, R. E., & Hoehn, M. M. (1969). Treatment of Parkinsonism With Levodopa. *JAMA Neurology*, 21(4), 343-354.
- Ye, Y., & Rape, M. (2009). Building ubiquitin chains: E2 enzymes at work. *Nature Reviews Molecular Cell Biology*, 10(11), 755-764.
- Yuan, L., Lv, Z., Atkison, J. H., & Olsen, S. K. (2017). Structural insights into the mechanism and E2 specificity of the RBR E3 ubiquitin ligase HHARI. *Nature Communications*, 8, 211.